Arteriosclerosis, Thrombosis, and Vascular Biology

ORIGINAL RESEARCH

Sotagliflozin Enhances Left Ventricular Function and Myocardial Perfusion in Chronic Myocardial Ischemia Through Metabolic and Redox Remodeling

Kelsey C. Muir, Christopher Stone, Riya Reddy, Meghamsh Kanuparthy, Jad Hamze, Dwight D. Harris, M. Ruhul Abid, Frank W. Sellke

BACKGROUND: Ischemic heart disease is the leading cause of mortality and human suffering globally. It often leaves patients with residual symptomatic burden despite current optimized procedural and medical options. Sotagliflozin, a dual SGLT1/2 (sodium-glucose cotransporter 1 and 2) inhibitor, has emerged for its clinically evident ischemic cardiovascular benefits. We hypothesize that sotagliflozin treatment exerts direct myocardial benefits in ischemic heart disease, independent of comorbid conditions.

METHODS: Yorkshire swine (n=22) underwent placement of an ameroid constrictor around the left circumflex coronary artery. Following a 2-week period in which the ameroid gradually closes, swine (n=18) were randomized to receive either 400 mg daily sotagliflozin (n=8) or no drug (n=10) for 5 weeks. Afterwards, swine underwent terminal harvest to acquire cardiac functional data with pressure-volume loops, myocardial perfusion by microsphere injection, and ventricular sectioning. To investigate the cellular and tissue-level impact of therapy, histology, immunoblotting, and high-throughput techniques were performed.

RESULTS: Sotagliflozin swine had improved ejection fraction, cardiac output, and stroke work compared with no drug ($P<0.05$) and a reduction in tau ($P=0.04$). Absolute blood flow to the ischemic myocardium was increased in the sotagliflozin group ($P=0.03$). Sotagliflozin swine had a reduction in 3-nitrotyrosine and trichrome staining, representing decreased reactive nitrogen species and myocardial fibrosis ($P=0.03$ for both). Molecularly, sotagliflozin swine demonstrated increased expression of endothelial nitric oxide synthase and superoxide dismutase 3 ($P=0.02$, $P=0.04$; respectively), with upregulated arginine metabolism, protein kinase A/cyclic adenosine monophosphate signaling, as well as glycolysis, fatty acid oxidation, and citric acid cycle.

CONCLUSIONS: Sotagliflozin treatment improved left ventricular function, myocardial perfusion, and diastolic relaxation, likely through reduced nitrosative stress and myocardial fibrosis, improved nitric oxide coupling, enhanced insulin signaling, and favorable metabolic shifts. This study suggests a potential role for sotagliflozin as a cardioprotective therapy in patients with ischemic heart disease beyond current treatment strategies.

Key Words: arginine ■ fibrosis ■ inflammation ■ insulin ■ perfusion

Ischemic heart disease (IHD) is the number 1 cause of morbidity and death globally.[1] Given the persistent burden on patients, providers, and society that IHD places, it becomes essential to urgently investigate targeted and cost-effective therapies. Current therapies rely heavily on guideline-directed medical therapy, which specifically originated for the treatment of heart failure rather than IHD, as well as procedural

Correspondence to: Kelsey C. Muir, Division of Cardiothoracic Surgery, Department of Surgery, Warren Alpert Medical School, Coro W 5.231, 1 Hoppin St, Providence, RI 02903. Email kelsey_muir@brown.edu
Supplemental Material is available at https://www.ahajournals.org/doi/suppl/10.1161/ATVBAHA.125.323916.
For Sources of Funding and Disclosures, see page XXX.

Arterioscler Thromb Vasc Biol is available at www.ahajournals.org/journal/atvb

Nonstandard Abbreviations and Acronyms

3-NT	3-nitrotyrosine
AMPK	5′ adenosine monophosphate-activated protein kinase
ANKRD	ankyrin repeat domain
ANP	atrial natriuretic peptide
CPT1β	carnitine O-palmitoyltransferase 1
eNOS	endothelial nitric oxide synthase
ERK1/2	extracellular signal-regulated kinase ½
FC	fold change
FHL1	four and a half LIM domain 1
GLUT4	glucose transporter 4
GPX3	glutathione peroxidase
HK2	hexokinase II
IHD	Ischemic heart disease
IL-4	interleukin 4
LCx	left circumflex coronary artery
NFκB	nuclear factor κ-light-chain-enhancer of activated B cells
NPPA	natriuretic peptide precursor A
p-eNOS	phosphorylated eNOS
PI3K	phosphoinositide 3-kinase
PICK1	PKA C-binding protein
PKA C	cAMP-dependent protein kinase catalytic subunit
SGLT	sodium-glucose cotransporter
SMAD2/3	mothers against decapentaplegic homolog 2/3
SOD3	superoxide dismutase 3
TCA	tricarboxylic acid
TGFβ	transforming growth factor β
TNFα	tumor necrosis factor α
α-SMA	alpha smooth muscle actin

What Are the Clinical Implications?

- Ischemic heart disease continues to leave patients with residual symptoms and progressive ventricular dysfunction despite current guideline-directed therapies. The current study provides new evidence that sotagliflozin may offer direct myocardial protection beyond its systemic glycemic effects. In a highly clinically relevant swine model of chronic ischemic heart disease, sotagliflozin improved left ventricular systolic function, diastolic relaxation, and perfusion to the ischemic myocardium, associated with reduced nitrosative stress, fibrosis, and inflammation. Our findings suggest the dual SGLT1/2 (sodium-glucose cotransporter 1 and 2) inhibition may directly support the ischemic myocardium and coronary microvascular function, even in the absence of comorbidities. Clinically, this project highlights the therapeutic potential of sotagliflozin in ischemic heart disease to not only stabilize cardiac performance but also delay progression toward heart failure. These insights provide strong evidence for future clinical trials evaluating sotagliflozin as a cardioprotective therapy in patients with ischemic heart disease, irrespective of comorbid status.

therapies, such as percutaneous coronary intervention or coronary artery bypass grafting.[2] However, gaps within the treatment guidelines persist not only because of the initial designation of medical therapy for patients with heart failure but also overlook a growing patient population with nonobstructive coronary artery disease, microvascular dysfunction, and incomplete revascularization. In fact, it was recently found that nonobstructive coronary artery disease is present in >50% of patients undergoing elective coronary angiography.[3] Furthermore, up to 30% of patients have incomplete revascularization following coronary artery bypass grafting, and similarly in 59% of patients following percutaneous coronary intervention.[4] These gaps within current treatment options for this extensive patient population, coupled with the significant and ever-rising health care burden of IHD, further illustrate the pressing need for more targeted and optimized medical therapy.

The recent development and success of SGLT2 (sodium-glucose cotransporter 2) inhibitors in heart failure further highlights the initial propensity towards this patient population, of which this drug class has become a cornerstone of guideline-directed medical therapy. For example, the CANVAS study found that canagliflozin reduced the risk of cardiovascular-related deaths and hospitalization due to heart failure compared with placebo, and this additionally was observed with empagliflozin in the EMPA-REG OUTCOME trial.[5,6] This resulted in the approval of these medications over the last 5 years by the Federal Drug Administration for the treatment of heart failure. Although importantly advancing the care of these patients, these medications failed to show benefit in patients suffering from ischemic cardiovascular disease, representing an important clinical precursor. This led to the promising studies investigating sotagliflozin, a dual SGLT1/2 inhibitor, in the SCORED trial and SOLOIST-WHF trial, which demonstrated a reduction in the risk of cardiovascular events and hospitalizations in patients with type II diabetes and heart failure.[7,8] Even more exciting was the secondary analysis of the SCORED trial, finding that sotagliflozin independently reduced ischemic cardiovascular events, such as myocardial infarction and stroke.[9] Since this ischemic-related benefit had not been previously shown with other drugs within its class, it raises the question whether dual SGLT1 and SGLT2 inhibition plays an important mechanistic role.

Furthering this notion was an important human-based study that revealed patients with heart failure have significant upregulation of the SGLT1 receptor within the left ventricular myocardium, which correlated with the degree of ventricular remodeling and overall systolic function of the heart.[10] Additionally, there have been growing hypotheses that SGLT2 inhibitors confer their cardioprotective effects via off-target SGLT1 inhibition and improved glycemic control, ultimately leading to less SGLT1 activation, reduction in reactive oxygen species production and intracellular sodium and calcium cytotoxicity, and the ability to more efficiently switch between metabolic substrates used by cardiomyocytes.[11,12] Currently, clear evidence is lacking on the molecular consequences of SGLT1 inhibition in the context of cardiovascular disease. Given emerging evidence that myocardial SGLT1 expression modulates disease and early clinical evidence of sotagliflozin-mediated ischemic cardioprotection, we aimed to investigate the effects and mechanisms of dual SGLT1/2 inhibition in a clinically relevant model of IHD. We hypothesize that sotagliflozin confers direct, comorbidity-independent, myocardial benefits in IHD, enhancing cardiac performance and mitigating maladaptive responses to chronic ischemia.

METHODS

The data that support the findings of this study are available from the corresponding author on reasonable request.

Protocol Overview

Yorkshire swine represent an ideal model to investigate cardiovascular disease and possible treatments, as swine have similar coronary distribution and cardiac physiology, lack preexisting collateralization, and share comparable myocardial proteome and metabolism to humans.[13,14] Another important aspect of our model was accurately accounting for sex as a biological variable; therefore, our 2 groups were matched by sex. Finally, based on prior experimental SD, β of 0.1, and an α of 0.05, we calculated an ideal sample size of ≈8 swine per group.

Our model began with 22 Yorkshire swine (CBSET, Lexington, MA) arriving at our facility at 10 weeks old, where they received a standard laboratory diet and were allowed to acclimate for 1 week. At 11 weeks old, they underwent placement of an ameroid constrictor around the proximal left circumflex coronary artery (LCx), as detailed previously.[15] Swine recovered for a 2-week period, which allowed time for the ameroid to gradually close, inducing chronic myocardial ischemia.[16] As described in our prior studies, the expected mortality rate is about 20%, which was observed in this project, with a majority of deaths caused by spontaneous ventricular arrhythmias due to premature ameroid closure.[15] Following this, 18 swine were randomized based solely on animal ID number and began treatment with either 400 mg of oral sotagliflozin daily (n=8, 5 female and 3 male) or no drug (control: n=10, 5 female and 5 male) for a total of 5 weeks. Finally, swine underwent a terminal harvest procedure in which cardiac function and myocardial perfusion measurements were acquired, as well as tissue collection.

Ameroid Procedure

The weight and length of each swine were obtained preoperatively. Swine received prophylactic antiplatelet therapy with aspirin (10 mg/kg), which continued for 5 days postoperatively, and a single intramuscular injection of antibiotics (Excede). Swine were anesthetized using intramuscular injections of Telazol (4.4 mg/kg) and xylazine (2.2 mg/kg) and subsequently intubated. Analgesia was provided with IV buprenorphine (0.03 mg/kg), and a fentanyl patch was placed (4 µg/kg). Swine were positioned in a modified right lateral decubitus position, and the left axillary region was properly prepped and draped. Anesthesia was maintained with inhaled isoflurane 0.75% to 3.0% throughout the procedure. A small left anterolateral thoracotomy was made to enter the chest in the second intercostal space. The left atrial appendage was retracted, and the left LCx was dissected free near its takeoff from the left main coronary artery. The LCx was isolated using a vessel loop. Following this, we conducted a gold microsphere injection to determine differential myocardial perfusion. Gold microspheres (5 mL) were injected into the left atrial appendage; meanwhile, the LCx was occluded by gentle retraction on the vessel loop and confirmed by ST-segment and T-wave changes on electrocardiography. The microspheres get lodged into the capillary beds and can later be quantified, which allows for the determination of the ischemic LCx territory and the nonischemic left anterior descending territory. Lastly, an appropriately sized ameroid constrictor, following visual evaluation of the artery, was placed around the proximal LCx. About 2 cm^3 of topical nitroglycerin was sprayed on the vessel to prevent vasospasm. The pericardium, chest wall, and skin were closed using absorbable sutures. Swine recovered in a padded area monitored by veterinary technicians, and as stated, were continued on daily aspirin for 5 days postoperatively.

Sotagliflozin Treatment

The swine experienced a 2-week recovery period. This time permitted the ameroid constrictor, which is made of a titanium outer ring and an inner casein hydrophobic core that absorbs bodily fluids, to gradually narrow and occlude the LCx. This mimics the gradual development of atherosclerosis in humans and represents initiating treatment when there is a diagnosis of IHD.

Following this period, swine were randomized using animal identification numbers to receive either 400 mg sotagliflozin daily or no drug (control). Sotagliflozin was administered orally in a treat. Given the rapid growth of adolescent swine, the treatment period lasted for a total of 5 weeks to maintain a similar heart-to-body weight ratio as human subjects. Additionally, regarding medication dosing, humans typically begin therapy with 200 mg of sotagliflozin for 2 weeks and uptitrate to 400 mg as tolerated.[17] The full 400 mg dose was selected in this preclinical study, as long as the swine tolerated the dosage, to ensure consistent and robust dual SGLT1/2 inhibition during a limited duration of treatment.

Terminal Harvest Procedure

Swine were weighed, and their length was measured preoperatively. Baseline blood glucose was obtained, and then a glucose tolerance test was performed using 0.5 g/kg of 50% dextrose

with blood glucose measurements taken at 30 and 60 minutes after administration. Swine were anesthetized and intubated in the same manner as the ameroid procedure. The swine were positioned supine and underwent a median sternotomy. The pericardium was opened, and any adhesions were lysed to expose the right and left atrial appendages. Pacing clamps were placed on both appendages attached to a single-chamber temporary pacemaker (OSCOR, Palm Harbor, FL). Additionally, the pleural space was entered to encircle and isolate the inferior vena cava with a vessel loop immediately before entering the pericardium.

Afterwards, a femoral groin cut-down was performed to expose the femoral artery. The femoral artery was dissected out with blunt and sharp dissection and isolated with vessel loops proximally and distally. Using the Seldinger technique, a 6F femoral artery sheath was placed. The sheath was connected to a blood withdrawal pump (Harvard Apparatus, Holliston, MA). Next, myocardial perfusion analysis was performed. Microspheres (5 mL) were injected into the left atrial appendage while simultaneously withdrawing blood from the pump at a rate of 6.67 mL/min. The microspheres used were lutetium at resting heart rate and then samarium when paced to 150 bpm (both from BioPAL, Worcester, MA). The following formula can be utilized to determine myocardial perfusion: (6.67 mL/min per weight of tissue [g])×(quantified tissue microsphere count/quantified blood reference microsphere count). Essentially, the ratio of quantified microspheres in the myocardial section to the quantified microspheres in the blood collected at a specific rate determines the blood flow to the myocardium.

Following this, a U-stitch was placed on the left ventricular apex. Using the Seldinger technique, another 6F arterial sheath was positioned within the ventricle, and a calibrated pressure-volume loop catheter was introduced (Millar, Houston, TX). Another catheter was placed into the femoral artery to obtain arterial pressures. The left ventricular catheter was secured, and pressure-volume loops were transmitted using the ADV500 Pressure-Volume Measurement System (Transonic, Ithaca, NY). Pressure-volume loops were recorded at resting heart rate during breath holds to limit respiratory variation and taken in sets of 3. This was repeated during inferior vena cava occlusions to determine preload-independent measurements as well as when paced to 150 bpm. This technique allowed for comprehensive hemodynamic characterization. Finally, cardiac euthanasia was performed to deliver the heart from the chest. The left ventricle was sectioned into 12 segments based on apical or basal position as well as proximity to the left anterior descending. The sections were either dried in preparation for microsphere quantification, fixed in 10% formalin for histological analysis, or snap-frozen in liquid nitrogen. Peripheral blood was sent to Rhode Island Hospital and analyzed for lipid profiling, liver function tests, and basic metabolic panel.

Immunofluorescence

After gold microsphere mapping, the most ischemic myocardial segments and nonischemic segments, previously fixed in 10% formalin for 24 hours and held in 70% ethanol, were sent to iHisto INC (Salem, MA) to be processed and embedded into formalin-fixed paraffin-embedded blocks. Additional frozen myocardial tissue was embedded in optimal cutting temperature compound blocks. Frozen and paraffin sections from ischemic myocardial blocks were then incubated with primary antibody to α-SMA (α-smooth muscle actin; Cell Signaling, with an appropriate isotype-matched negative control) and Isolectin B4 (Cell Signaling, with an omission negative control) to determine arteriolar and capillary density, respectively. 4′,6-diamidino-2-phenylindole was used as a nuclear counterstain. Whole slide imaging was performed by iHisto using the Pannoramic Midi II (Budapest, HU). This was followed by quantification by unaffiliated iHisto technicians using HALO Area Quantification FL (Indica Labs, Albuquerque, NM).

Immunohistochemistry

Sections from the same ischemic myocardial formalin-fixed paraffin-embedded and optimal cutting temperature blocks were used for 3-nitrotyrosine (3-NT) and trichrome staining to quantify reactive nitrogen species and myocardial fibrosis, respectively. A positive control with known collagen content was performed for trichrome staining to ensure appropriate staining. The blocks were also incubated with Fabgennix SGLT1 Polyclonal Antibody (Thermo Fisher Scientific, catalog number: SGLT-112AP). In addition, fresh frozen sections of kidney tissue from control and sotagliflozin swine were made into optimal cutting temperature blocks and incubated with the same SGLT1 Polyclonal Antibody as well as Fabgennix SGLT2 Polyclonal Antibody (Thermo Fisher Scientific, catalog number: SGLT2-201AP). Both SGLT1 and SGLT2 antibodies underwent a validation process by iHisto technicians, including negative controls, to determine the appropriate antibody concentration and ensure antibody specificity. Whole slide imaging was conducted by iHisto utilizing the Pannoramic Midi II (Budapest, HU), and positive-area quantification was performed by unaffiliated iHisto technicians with HALO Area Quantification Brightfield (Albuquerque, NM).

Immunoblotting

After gold microsphere quantification determined the most ischemic segment, lysates were produced from this myocardium by homogenizing the tissue with RIPA and Extraction Buffer and Halt Protease Inhibitor Cocktail (Thermo Fisher Scientific, Franklin, MA). A BCA Protein Assay Kit was used to measure protein concentration, followed by 40 µg of lysate being run on a 4% to 12% Bis-Tris gel and transferred to nitrocellulose (all from Thermo Fisher Scientific, Franklin, MA). Membranes were blocked with 5% nonfat dry milk for 1 hour and incubated in primary antibody dilutions (1:1000 in 5% BSA) for 24 hours. Horseradish peroxidase-conjugated secondary antibodies (anti-mouse or anti-rabbit, Cell Signaling, Danvers, MA) were diluted 1:2000 in 3% BSA and incubated for 1 hour at room temperature. Membranes were then imaged using a ChemiDoc Imaging System (Bio-Rad, Hercules, CA) and ECL Western blotting Substrate (Thermo Fisher Scientific, Franklin, MA) as the developing reagent. Membranes were stripped using Restore PLUS Western Blot Stripping Buffer (Thermo Fisher Scientific, Franklin, MA) for repeat probing. Membranes were normalized to vinculin or GAPDH (Cell Signaling, Danvers, MA) for any loading variation. Immunoblot data were analyzed using ImageJ software (National Institutes of Health, Bethesda, MD). Figure S1 depicts the unedited, analyzed immunoblots.

Oxyblot

Oxidative stress within the ischemic myocardial tissue was assessed using the OxyBlot Protein Oxidation Detection Kit (MilliporeSigma, Burlington, MA), which detects protein carbonylation. Lysates from above were used, in which 20 µg of protein was denatured, derivatized with 2,4-dinitrophenylhydrazine for 15 minutes at room temperature, and neutralized per the manufacturer's instructions. Samples were resolved on a 4% to 12% Bis-Tris gel, transferred to a nitrocellulose membrane, and probed with kit-provided primary and secondary antibodies. Protein oxidation was visualized via chemiluminescence (Bio-Rad ChemiDoc MP, Hercules, CA) and quantified by densitometric analysis using ImageJ software (National Institutes of Health, Bethesda, MD).

Proteomics

Ischemic myocardial tissue lysates (n=4/group) were created via sonification in 10% SDS and 50 mmol/L of triethylammonium bicarbonate and further processed and analyzed by the Brown University Proteomic Core. Protein digestion was performed using S-Trap Micro columns (ProtiFi, Fairport, NY) with minor adjustments. Lysates were reduced with dithiothreitol, alkylated with iodoacetamide, acidified with 2.5% phosphoric acid, and precipitated with cold methanol and triethylammonium bicarbonate before loading onto columns. Following washes, proteins were digested overnight with trypsin, and peptides were sequentially eluted, vacuum-dried, and reconstituted in 0.1% formic acid with indexed retention time peptides (Biognosys, Ki-3001-1) for retention time alignment.

Peptides were analyzed by both data-independent acquisition and data-dependent acquisition LC-MS using a Vanquish Neo UHPLC and Orbitrap mass spectrometer. Data-independent acquisition was conducted with a 60-minute C18 gradient, 40 overlapping windows, and Orbitrap detection at 30k resolution. Data-dependent acquisition used the same gradient with dynamic exclusion and turbo ion trap detection. Raw files were analyzed in Spectronaut (v19.6) with a 1% FDR threshold at protein spectrum match, peptide, and protein levels. Spectral libraries were generated against the Sus scrofa UniProt database (UP000008227_9823_20251105, 22781 entries) with standard variable and fixed modifications. Protein intensities were normalized to total sample intensity in Excel and analyzed for $\log_2$ (fold change [FC]) and Student *t* test. Individual proteins were deemed significant if $\log_2$ (FC)>0.5 or <–0.5 and a $P<0.05$.

Metabolomics

Frozen sections of the most ischemic myocardial tissue from both groups were given to the Dana Farber Metabolomic Core Facility. First, myocardial tissue was homogenized in cold extraction solvent (70% [v/v] ethanol) and polar metabolites extracted using hot extraction solvent. Untargeted metabolite analysis was conducted using a QExactive HF-X mass spectrometer and coupled to a Vanquish binary UPLC system (Thermo Fisher Scientific, Waltham, MA). The analytes were ionized via a HESI II probe. Two chromatographic separations were performed for each sample. In both, 5 µL of sample was injected into a BEH Z-HILIC column (100×2.1 mm, 1.7 µm, Waters) with the first separation being performed with 15 mmol/L ammonium bicarbonate (Merck) in 90% water and 10% acetonitrile as mobile phase A, and mobile phase B was 15 mmol/L ammonium bicarbonate in 95% acetonitrile and 5% water. The chromatographic gradient was adapted from prior work and was carried out at a flow rate of 0.225 mL/min.[18] This mass analysis was carried out in negative mode. The second separation was adapted from Mülleder et al.[19] Both mobile phases A and B were buffered with 10 mmol/L ammonium formate and 45 mmol/L formic acid (pH 2.7). In mobile phase A, the solvents were in 1:1 acetonitrile:water, and in mobile phase B, they were 95:5:5 acetonitrile:water:methanol. The column oven was held at 40 °C and the autosampler at 4 °C. The chromatographic gradient was run at a flow rate of 0.4 mL/min as follows: 0.75 minute initial hold at 95% B; 0.75 to 3.00 minutes linear gradient from 95% to 30% B, 1.00 minute isocratic hold at 30% B. B was brought back to 95% over 0.50 minutes, after which the column was re-equilibrated under initial conditions. Metabolites were analyzed in positive mode.

Sample acquisition was conducted in full-scan mode, with the spray voltage set to 3 kV (negative) or 3.5 kV (positive), the capillary temperature to 320 °C, the HESI probe to 300 °C, sheath gas to 40U, AUX gas to 8U, sweep gas to 1 unit, and resolving power to 120 000. An untargeted metabolite library was created via top-15 data-dependent acquisition acquisitions were performed on a pooled study sample. MS1 resolution was set to 60 000 and MS2 to 30 000. The raw data files were processed using MZmine 3 and Emzed.[20,21] The Metabolite MS2 spectra were compared with HMDB, GNPS, Massbank, and MoNA databases using Spectral library search (ref to data-dependent acquisition _library). In addition, retention times and m/z values of a full-scan acquisition on a pooled study sample were compared with an in-house database of retention times determined for authentic standards (Human Endogenous Metabolite Compound Library Plus L2501, TargetMol, Wellesley, MA). Internal standards were integrated using Emzed, and raw peak areas were normalized by dividing by sample biomass and the mean internal standard area. The data was then analyzed for (1) internal standard and biomass normalized peak areas and (2) just biomass normalized peak areas to calculate statistics (Welch *t* test and $\log_2$fold change) between all groups for each metabolite. The 2 methods were conducted because the internal standards were poorly detected. Using this database, enrichment and network analysis were subsequently performed using MetaboAnalyst 6.0.[22] Individual metabolites were deemed significant with a $\log_2$ (FC) of > 0.5 or <–0.5 and a $P<0.05$.

Pathway Integration of Proteomic and Metabolomic Data Sets

Subsequently, the untargeted metabolomic and proteomic data sets were integrated using MetaboAnalyst's Joint Pathway Analysis tool to identify pathways affected by our experimental therapy. Because many m/z features detected in untargeted metabolomics cannot be confidently annotated due to spectral library limitations, mummichog was employed, an algorithm that enables pathway enrichment analysis directly using peak data (m/z and retention time pairs) without requiring prior metabolite identification.[23] This method leverages the tendency of related metabolites to covary within biological pathways, assigning putative KEGG compound IDs for pathway-level interpretation. The integrated

data was then visualized using iPath 3.0 to generate interactive metabolic maps.[24] In these visualizations, all detected features were overlaid onto pathway maps, regardless of statistical enrichment, to provide a comprehensive overview of pathway-level changes. Color coding in iPath visualizations reflects the directionality of change, in which blue indicates downregulation and red indicates upregulation.

Statistical Analysis

Prism 10 (GraphPad Software, San Diego, CA) was used to complete the statistical analysis. Of note, researchers were blinded to the experimental group when analyzing the hemodynamic parameters and myocardial perfusion. Initially, data were assessed for outliers using the ROUT method, and normality was tested using the Shapiro-Wilk test. Nonparametric data were evaluated using the Mann-Whitney *U* test, while normally distributed data with homogenous variances were analyzed using the unpaired Student *t* test. The relationship between SGLT1 expression and perfusion was assessed using Pearson correlation analysis.

Finally, the control and sotagliflozin groups were subdivided by sex to determine any sex-based differences in overall cardiac function and myocardial perfusion. For this analysis, a 2-way ANOVA was used (factors: treatment and sex), followed by Sidak post hoc multiple comparisons test. A $P<0.05$ was deemed statistically significant.

Study Approval

All experiments were approved by the Institutional Animal Care and Use Committee of Brown University (protocol number 23-08-0005), and the surgical procedures and animal care were conducted in accordance with the National Institutes of Health Guide for the Care and Use of Laboratory Animals and Principles of Laboratory Animal Care.

RESULTS

Biochemical and Physiological Metrics

There was no difference between the sotagliflozin and control groups in regard to body mass index at the time of the ameroid procedure, the harvest procedure, or change in body mass index between the 2 procedures (all $P>0.05$; Table 1). There was no significant difference in baseline blood glucose at the time of the harvest procedure; however, there was improvement in glucose tolerance testing in the sotagliflozin-treated swine compared with control swine at both 30 and 60 minutes after dextrose administration ($P<0.0001$ for both). There were no significant differences in liver function testing, triglyceride level, or C-reactive protein between groups. There was an increase in albumin and total cholesterol in the sotagliflozin group compared with control ($P=0.04$ for both), and a nonsignificant increase in low-density lipoprotein cholesterol ($P=0.07$; Table 1). Of note, a mild increase in cholesterol and low-density lipoprotein levels has been widely seen in human patients after SGLT2 inhibitor treatment.[25]

Table 1. Biochemical and Metabolic Parameters Presented With Mean±SEM; Variables Analyzed Using an Unpaired *t* Test or Mann-Whitney *U* Test

Metabolic parameter	CON (n=10)	SOT (n=8)	*P* value
BMI at ameroid, kg/m^2	54.7±2.5	53.5±1.7	0.72
BMI at harvest, kg/m^2	68.5±1.8	69.8±3.5	0.72
% change in BMI	18.6±4.7	22.5±3.2	0.52
Baseline BG, mg/dL	80.7±4.2	70.1±2.4	0.06
BG at 30 min, mg/dL	202.2±16.5	131.9±3.6	<0.0001*
BG at 60 min, mg/dL	186.2±9.7	108.5±5.4	<0.0001*
Albumin, g/dL	2.5±0.1	2.7±0.04	0.04†
Total protein, g/dL	4.7±0.2	5.0±0.2	0.16
Total bilirubin, mg/dL	0.1±0.01	0.1±0.02	0.41
Alkaline phosphatase, IU/L	151.8±16.1	140.4±9.4	0.59
ALT, IU/L	67.4±3.9	83.1±7.7	0.07
AST, IU/L	23.4±2.2	23.9±1.8	0.88
C-reactive protein	0.26±0.03	0.3±0.03	0.79
Triglycerides, mg/dL	10.5±1.4	8.5±0.5	0.62
Total cholesterol, mg/dL	65.7±2.9	78.0±4.8	0.04†
HDL, mg/dL	35.0±2.1	38.5±2.2	0.27
LDL, mg/dL	30.4±2.1	36.9±2.7	0.07

There was no difference in BMI between SOT and CON swine. Glucose tolerance testing demonstrated improved glucose handling of SOT swine. The SOT group had increased total cholesterol and albumin, as well as a nonsignificant increase in LDL levels, compared with CON. CON (n=10; 5 male, 5 female) and SOT (n=8; 5 female, 3 male). ALT indicates alanine aminotransferase; AST, aspartate aminotransferase; BG, blood glucose; BMI, body mass index; CON, control; HDL, high-density lipoprotein; LDL, low-density lipoprotein; and SOT, sotagliflozin.

Sotagliflozin Treatment Augmented Overall Systolic and Diastolic Cardiac Function

There were no differences in either heart rate or mean arterial pressure between the sotagliflozin-treated swine and control ($P=0.14$, $P=0.4$; respectively; Table S1).

Resting Data

The sotagliflozin group had improved systolic function, as evident by increased ejection fraction, stroke work, cardiac output, and minimum derivative of volume compared with the control group (all $P<0.05$; Figure 1). Sotagliflozin swine demonstrated improved minimum derivative of pressure and maximum power ($P=0.03$, $P=0.05$; respectively). Additionally, sotagliflozin-treated swine had enhanced diastolic function determined by a reduction in the isovolumic relaxation constant compared with control swine ($P=0.04$) as well as an increase in the maximum derivative of volume ($P=0.01$; Figure 1). These findings indicate improved myocardial contractility and left ventricular efficiency during systole as well as augmented ventricular compliance. There were no differences between sotagliflozin and control in end-systolic pressure volume relationship, end diastolic or systolic volume, preload recruitable stroke work, maximum derivative of pressure, arterial elastance, or pressure volume area (Table S1).

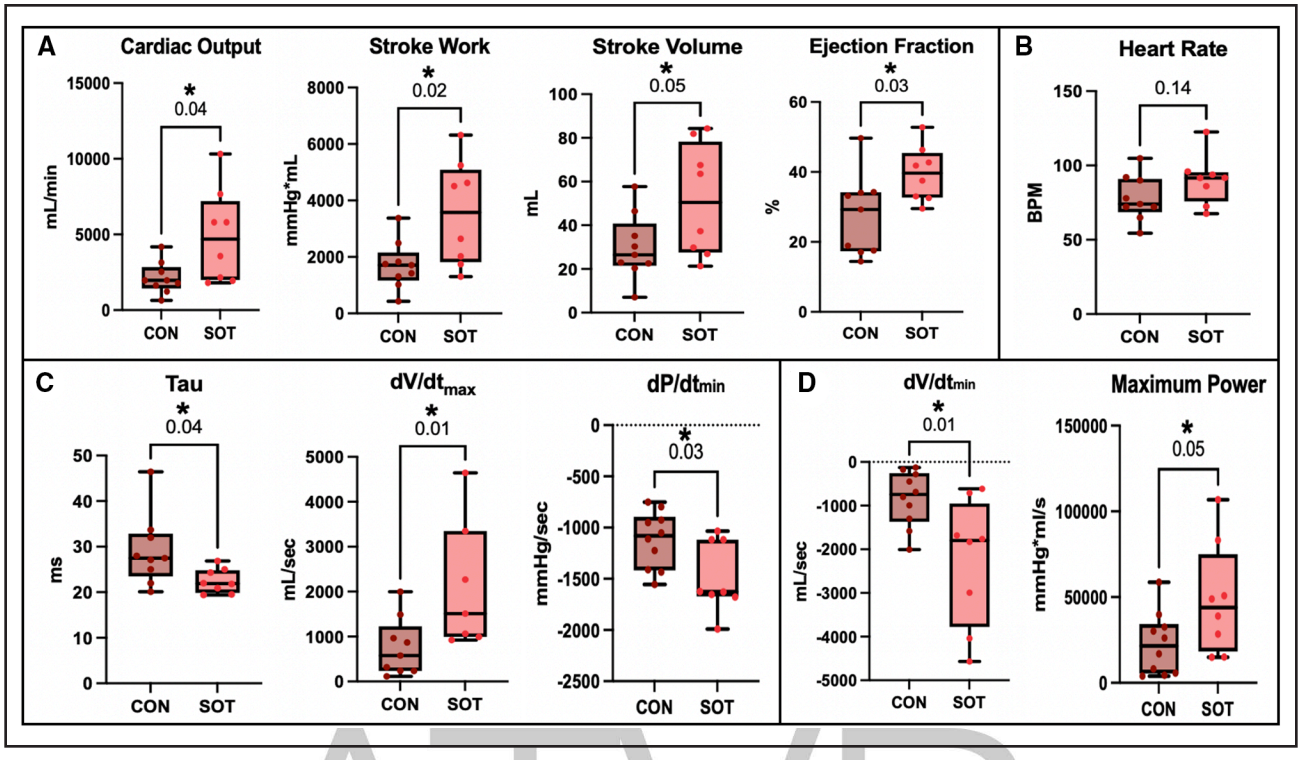

Figure 1. Sotagliflozin (SOT) improved systolic and diastolic cardiac function at rest.
A, SOT (n=8; 5 female and 3 male) demonstrated improved systolic functional parameters, including stroke work, cardiac output, and ejection fraction compared with control (CON, n=10; 5 female and 5 male). **B**, There was no difference in heart rate between groups (P=0.14). **C**, SOT demonstrated significantly reduced tau, increased maximum derivative of volume (dV/dt_{max}), and lower (more negative) minimum derivative of pressure (dP/dt_{min}) compared with CON, illustrating improved diastolic relaxation. **D**, SOT swine had improved dV/dt_{min} and maximum power compared with CON, illustrating improved left ventricular power and efficiency. Each variable was analyzed by an unpaired t test (parametric data) or Mann-Whitney U test (nonparametric data). *P<0.05.

When the 2 groups were subdivided by sex, there were no significant sex-based differences observed in ejection fraction, stroke work, SV, cardiac output, minimum derivative of volume, maximum derivative of volume, or isovolumic relaxation constant, suggesting minimal cardiac functional sex-based differences in response to treatment (all P>0.05).

Paced Data

Sotagliflozin swine had increased stroke work and maximum power when paced to 150 bmp compared with control (P=0.04, P=0.02; respectively). There were no differences in ejection fraction, SV, cardiac output, or left ventricular end diastolic volume between the sotagliflozin and control swine (Table 2).

Treatment With Sotagliflozin Increased Myocardial Perfusion to the Ischemic Territory Without Impacting Collateralization Formation

Swine treated with sotagliflozin had increased blood flow to the chronically ischemic myocardium at rest when compared with controls (P=0.03); however, this was not observed when paced to 150 bpm (P=0.97; Figure 2A). When subdivided by sex, there was no significant difference in resting myocardial perfusion to the ischemic territory (P=0.1). Additionally, there was a nonsignificant increase in blood flow at rest to the nonischemic

Table 2. Invasive Hemodynamic Parameters Obtained Via Pressure-Volume Loop Catheterization When the Heart Was Paced to 150 bpm

Hemodynamic parameter	CON (n=10)	SOT (n=8)	P value
Ejection fraction, %	19.4±3.3	26.5±2.9	0.15
Stroke volume, mL/beat	20.8±5.2	25.5±5.4	0.54
Stroke work, mm Hg·mL	842.1±211.7	1726±369.2	0.04*
Cardiac output, mL/min	3109±779.5	3784±802	0.56
LV end-diastolic volume, mL	84.2±16.8	87.7±9.5	0.86
dV/dt_{max}, mL/s	1120±171.1	1169±179.5	0.95
dV/dt_{min}, mL/s	−951.5±117.4	−1914±605.8	0.16
Maximum power, mm Hg·mL/s	28408±6314	67859±13316	0.02*
Pressure volume area, mm Hg·mL	25140±20065	103565±88919	0.45

Presented as mean±SEM; variables analyzed using an unpaired t test or Mann-Whitney U test. SOT swine had improved maximum power when compared with CON. CON (n=10; 5 male, 5 female) and SOT (n=8; 5 female, 3 male). CON indicates control; dV/dt, derivative of volume; LV, left ventricular; and SOT, sotagliflozin.

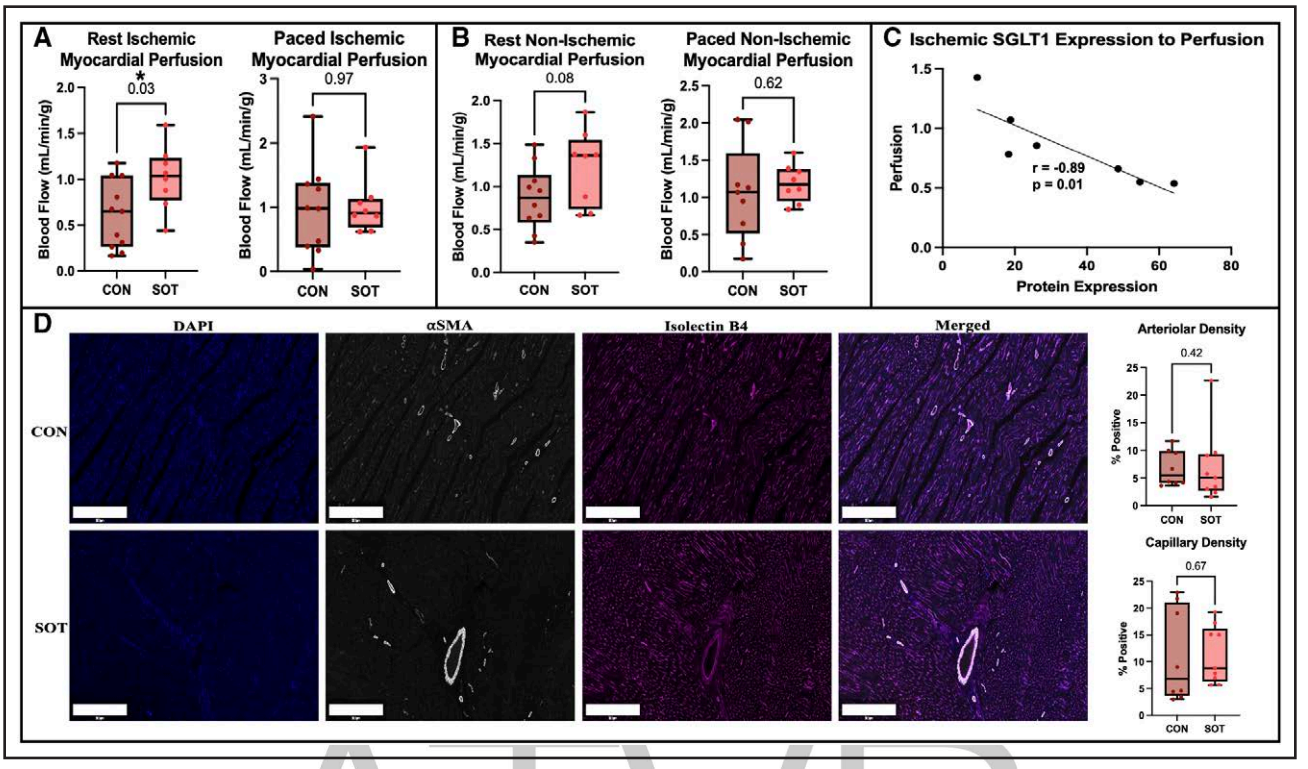

Figure 2. Sotagliflozin (SOT) increases perfusion to the ischemic myocardium without increasing collateral density. **A**, In the ischemic territory, absolute myocardial blood flow at rest was higher in SOT swine (n=8; 5 female and 3 male) than in control (CON, n=10; 5 female and 5 male); this difference was attenuated during pacing. Blood flow was determined by microsphere injection at the time of harvest and analyzed by *t* test. **B**, In the nonischemic territory, absolute myocardial blood flow was similar between groups, with a nonsignificant increase in perfusion at rest in SOT. The variables were analyzed by *t* test. **C**, Correlation between ischemic myocardial SGLT1 (sodium-glucose cotransporter 1) expression in SOT-treated swine and ischemic-to-nonischemic perfusion ratio. SOT swine demonstrated a strong negative correlation between SGLT1 expression and perfusion. Correlation analysis was performed using Pearson correlation in Prism 10. **D**, Representative immunofluorescence staining (4′,6-diamidino-2-phenylindole [DAPI], α-SMA [α-smooth muscle actin] for arterioles, Isolectin B4 for capillaries) and quantification show no difference in arteriolar or capillary density in the ischemic zone between groups. Scale bars represent 500 µm. Analysis was performed by an unpaired *t* test. **P*<0.05.

myocardium supplied by the left anterior descending when comparing the sotagliflozin-treated swine to the control (*P*=0.08); meanwhile, there was no difference when paced to 150 bpm (*P*=0.62; Figure 2B). Moreover, the ratio of ischemic myocardial perfusion to nonischemic perfusion at rest was significantly increased in the sotagliflozin swine (*P*=0.01), normalizing for systemic flow variations, and indicating improved relative perfusion to the ischemic territory. On immunofluorescence, sotagliflozin swine showed no significant changes in arteriolar density or capillary density within the ischemic myocardium compared with control (*P*=0.42, *P*=0.67; respectively; Figure 2D).

Sotagliflozin Augmented Nitric Oxide and Vascular Reactivity Pathways in Ischemic Myocardium

Sotagliflozin-treated swine demonstrated alterations in the expression of enzymes involved in nitric oxide production and vascular reactivity. On immunoblotting, sotagliflozin swine were found to have increased expression of eNOS (endothelial nitric oxide synthase; *P*=0.02). However, there was no difference in p-eNOS (phosphorylated eNOS) between the 2 groups (*P*=0.60), and therefore, there was an observed nonsignificant reduction in the ratio of p-eNOS to eNOS among the sotagliflozin-treated swine (*P*=0.06; Figure 3B). On proteomic analysis, the increased expression of eNOS did not reach statistical significance between the 2 groups. Interestingly, there was significant upregulation of NPPA (natriuretic peptide precursor A; $\log_2$ (FC)=1.67, *P*=0.0008), which is converted into ANP (atrial natriuretic peptide; Figure 3A). Although widely known for its systemic effects on natriuresis and blood pressure, ANP can have substantial local and regional effects on myocardial vascular tone and volume, as well as beneficial effects on fibrosis and maladaptive remodeling.[26]

Furthermore, pathway enrichment of the metabolomic data set demonstrated significant augmentation of arginine and proline metabolism (Figure 3D). Arginine is the primary precursor for nitric oxide production within the vascular endothelium; therefore, an increase in arginine levels, as well as its metabolism,

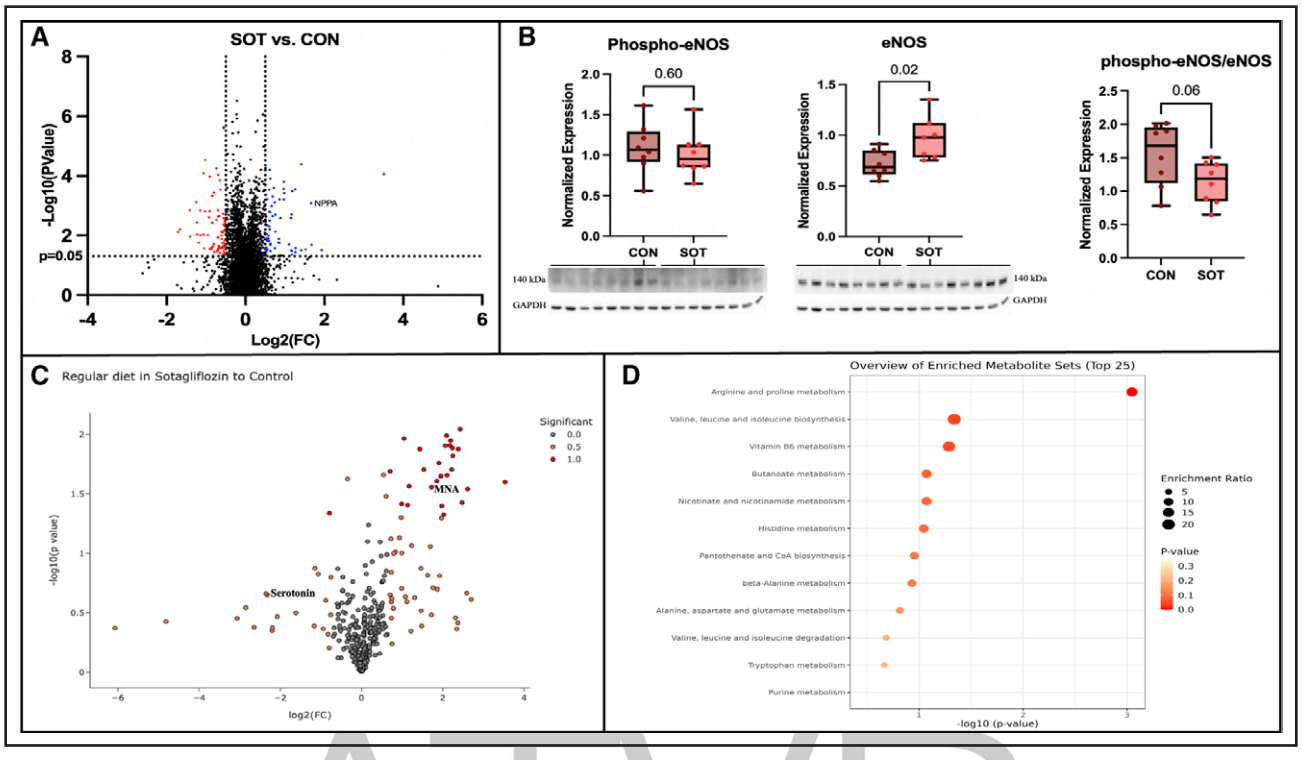

Figure 3. Molecular correlates of vascular reactivity in sotagliflozin (SOT)-treated swine.
A, Global proteomic volcano plot (log_2FC vs -log10p-value) comparing SOT vs control (CON). Proteins upregulated in the SOT swine are highlighted in blue; notably, NPPA (precursor of atrial natriuretic peptide [ANP]) was upregulated, a peptide with recognized effects on myocardial vascular tone and antifibrotic signaling. **B**, Immunoblot quantification demonstrates increased expression of endothelial nitric oxide synthase (eNOS) in SOT swine vs CON, accompanied by a lower phosphorylated eNOS to eNOS ratio. Representative blots are shown (normalized to loading control). Findings were concordant with proteomic analysis. Analysis was performed using an unpaired *t* test. **C**, Untargeted metabolomic volcano plot. A scoring system was applied because of the untargeted nature of the analysis, in which log2 (FC) of 0.5 or −0.5 gets 0.5 points, and $P<0.05$ adds another 0.5 points. The dark red dots demonstrate metabolites with a score of 1.0; notably, 1-methylnicotinamide (MNA), a metabolite that has been reported to enhance endothelial function. **D**, MetaboAnalyst metabolite-set enrichment highlights pathways increased in SOT, including arginine and proline metabolism, illustrating a key precursor for nitric oxide production within the vascular endothelium. Dot size reflects enrichment ratio, and position reflects $-log_{10}$ (*P* value). SOT (n=8 with 5 female and 3 male); CON (n=8 with 4 male and 4 female).

likely indicates an increased production of nitric oxide. Additionally, there were decreased levels of serotonin in the sotagliflozin-treated swine (log2 [FC]=−2.4), although this did not reach statistical significance (P=0.21). Given the recent and novel metabolomic study demonstrating that human subjects with IHD had significantly elevated levels of serotonin as well as its known vasoconstrictive effects, it is worth mentioning such a decrease in levels after treatment.[27] This balance of increased arginine metabolism and decreased serotonin levels suggests improved endothelial function and vascular reactivity.

Lastly, levels of 1-methylnicotinamide were significantly elevated in the sotagliflozin swine (log2 [FC]=1.2; P=0.03), a metabolite that has been implicated in exerting antithrombotic and anti-inflammatory effects as well as improved vascular reactivity (Figure 3C). Studies have demonstrated that methylnicotinamide restored reactive oxygen species-associated endothelial dysfunction by normalizing eNOS function and increasing NO bioavailability within the endothelium.[28]

Sotagliflozin Altered Key Signaling Pathways Likely Due to SGLT1 Inhibition

Both control and sotagliflozin-treated swine demonstrated global SGLT1 staining of the left ventricular myocardium. Within the ischemic myocardium, there was no difference in cotransporter abundance between the 2 groups (P=0.4; Figure 4B). However, sotagliflozin swine demonstrated a strong negative correlation between ischemic territory SGLT1 receptor expression and the ischemic/nonischemic perfusion ratio (r=−0.89, P=0.01; Figure 2C). Additionally, SGLT1 was significantly reduced in the nonischemic territory in sotagliflozin-treated swine (P=0.02; Figure 4A).

As determined by immunoblotting, sotagliflozin therapy was associated with the reduction of phosphorylated AMPK (5′ adenosine monophosphate-activated protein kinase) without differences in expression of AMPK (P=0.02, P=0.24; respectively). The ratio of phosphorylated AMPK to AMPK was therefore significantly reduced after sotagliflozin treatment (P=0.003;

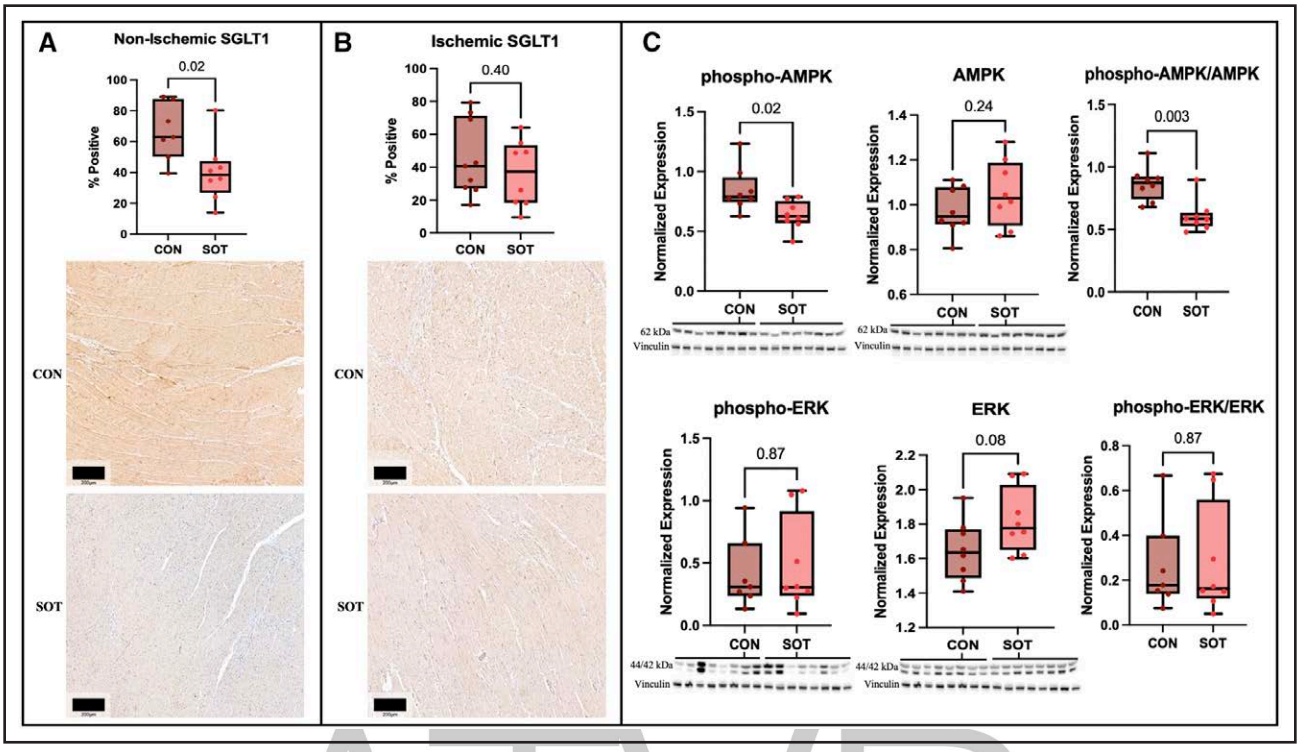

Figure 4. SGLT1 (sodium-glucose cotransporter 1) expression and AMPK (5' adenosine monophosphate-activated protein kinase)/ERK (extracellular signal-regulated kinase) signaling.
A, Nonischemic myocardium: SGLT1 immunohistochemistry shows reduced expression in sotagliflozin (SOT) swine vs control (CON). **B**, Ischemic myocardium: SGLT1 staining is comparable between groups. Representative images are shown (scale bars: 200 µm). **C**, Immunoblot analysis of key signaling pathways. Phospho-AMPK and the phospho-AMPK/AMPK ratio are reduced in SOT, whereas total AMPK is unchanged. Total ERK1/2 shows a nonsignificant increase in SOT, with no difference in phospho-ERK1/2 or the phospho-ERK/ERK ratio. Representative blots and box-and-whisker quantification are shown with *P* values indicated; protein levels were normalized to a loading control. SOT (n=8 with 5 female and 3 male); CON (n=8 with 4 male and 4 female). Each variable was analyzed by an unpaired *t* test (parametric data) or Mann-Whitney *U* test (nonparametric data).

Figure 4C). This was corroborated by proteomic analysis, in which there were no protein expression changes between groups in all 3 subunits that directly comprise AMPK. Additionally, immunoblotting and proteomic analysis demonstrated no difference in expression of ERK1/2 (extracellular signal-regulated kinase 1/2) nor the PI3K (phosphoinositide 3-kinase)/Akt pathway. Immunoblotting revealed no changes in phosphorylation of ERK1/2 between the 2 groups (*P*=0.87; Figure 4C).

Furthermore, sotagliflozin swine were found to have increased expression of cAMP-dependent PKA C (protein kinase catalytic subunit) on immunoblotting (*P*=0.004). There was no difference in phosphorylation of PKA C between groups (*P*=0.62). Additionally, proteomic analysis revealed increased expression of PICK1 (PKA C-binding protein; $\log_2$ [FC]=0.52, *P*=0.02), which is a scaffolding protein essential for anchoring PKA C to the membrane. On metabolomic analysis, cAMP was observed to be increased in the sotagliflozin-treated swine, which is a key cardiac second messenger for improvement in excitation-contraction coupling ($\log_2$ [FC]=0.6, *P*=0.03).[29]

Sotagliflozin Reduced Nitrosative Stress and Increased Antioxidant Enzymes Within the Ischemic Myocardium

Sotagliflozin therapy was associated with a reduction in 3-NT staining within the ischemic myocardium when compared with control (*P*=0.03), representing a reduction in reactive nitrogen species (Figure 5A). On proteomic analysis, sotagliflozin treatment was associated with increased expression of SOD3 (superoxide dismutase 3; $\log_2$ [FC]=0.5, *P*=0.04) as well as GPX3 (glutathione peroxidase; $\log_2$ [FC]=0.55, *P*=0.0006). SOD3 acts mainly on superoxide, which would effectively reduce the formation of peroxynitrite that is detected by 3-NT. Of note, there was no significant difference in overall oxidative stress, as determined by OxyBlot, between the sotagliflozin and control swine (*P*=0.81; Figure 5B). Given that OxyBlot detects protein carbonylation, a general marker of reactive oxygen species damage, the summation of these findings suggests a more nuanced and selective modulation of oxidative stress within the myocardium.

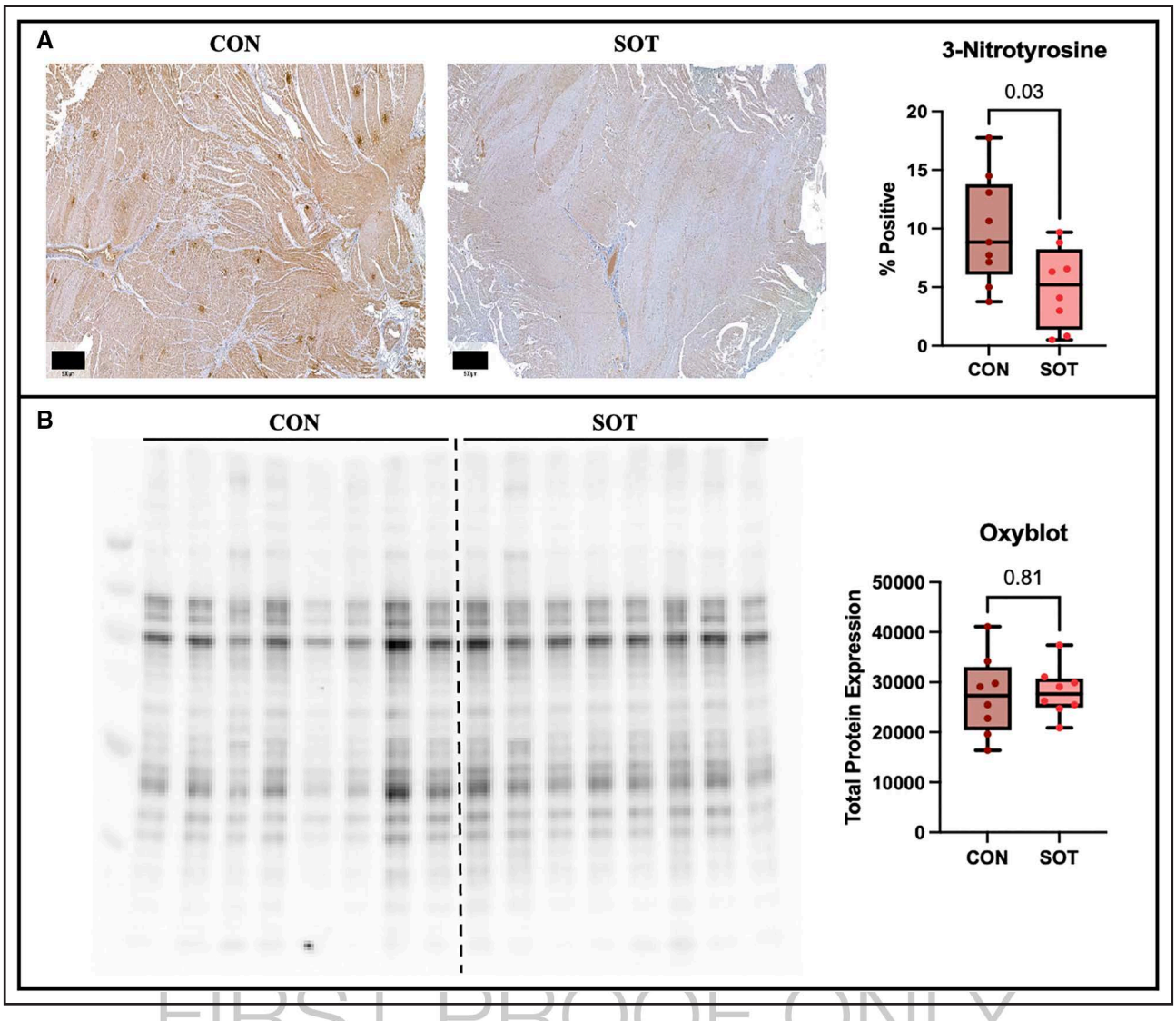

Figure 5. Nitro-oxidative stress in the ischemic myocardium.
A, Immunohistochemistry for 3-nitrotyrosine (3-NT) demonstrates decreased staining in sotagliflozin (SOT) vs control (CON, *P*=0.03), consistent with reduced nitrosative stress. Scale bars=500 µm. **B**, Protein carbonylation (OxyBlot) shows no difference in total carbonyl signal between groups (*P*=0.81). Representative images/blots and box-and-whisker quantification are shown with *P* values indicated. SOT (n=8 with 5 female and 3 male); CON (n=8 with 4 male and 4 female). Each variable was analyzed by an unpaired *t* test (parametric data) or Mann-Whitney *U* test (nonparametric data).

Sotagliflozin Treatment Reduced Myocardial Fibrosis and Inflammation Within the Ischemic Myocardium

Sotagliflozin swine were found to have a reduction in trichrome staining within the ischemic myocardium compared with control, demonstrating a reduction in fibrosis (*P*=0.03; Figure 6A). Well-established profibrotic signaling was unchanged, with no difference in expression of TGFβ (transforming growth factor β) or SMAD2/3 (mothers against decapentaplegic homolog 2/3) by immunoblot (*P*=0.72, *P*=0.33; respectively; Figure 6B). However, inflammatory mediators were attenuated; NFκB (nuclear factor κB) p65 subunit and interleukin-4 (IL-4) were reduced in sotagliflozin (*P*=0.02, *P*=0.04; respectively; Figure 6C), concordant with proteomic analysis showing a reduction in NFκB p100 subunit (NFκB2; $\log_2$ [FC]=−0.50, *P*=0.04). There was no difference in expression of IL (interleukin) 1β or TNFα (tumor necrosis factor α) between groups (*P*=0.15, *P*=0.76; respectively). Additionally, proteomic analysis revealed sotagliflozin swine had decreased expression of FHL1 (four and a half LIM domain 1; $\log_2$ [FC]=−1.25, *P*=0.0008), and ANKRD1/ANKRD2 (ankyrin repeat domain 1 and 2; $\log_2$ [FC]=−1.01, −1.05, *P*=0.00003, *P*=0.03; respectively). FHL1 is a scaffolding protein that has been implicated in cardiac remodeling and hypertrophy, and ANKRD1/2 are stress-responsive proteins that have also been linked to maladaptive cardiac hypertrophy and fibrosis associated with cardiomyopathy.[30,31]

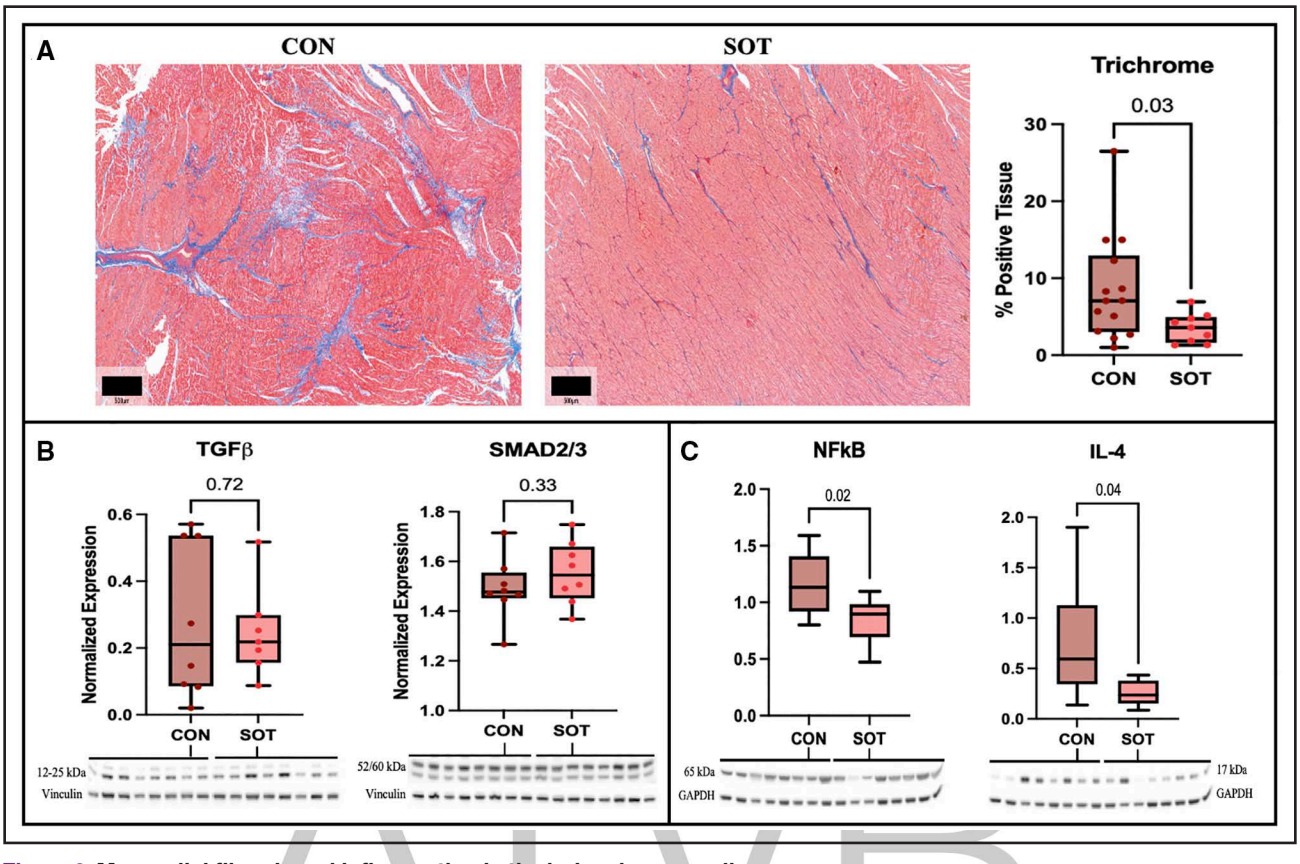

Figure 6. Myocardial fibrosis and inflammation in the ischemic myocardium.
A, Immunohistochemistry of trichrome staining illustrates reduced myocardial fibrosis within the ischemic territory in the sotagliflozin (SOT) group compared with control (CON). Scale bars=500 µm. **B**, Immunoblotting depicts no difference in TGFβ (transforming growth factor β)/SMAD2/3 (mothers against decapentaplegic homolog 2/3) expression between the 2 groups. **C**, Immunoblot analysis revealed reduced expression of NFκB (nuclear factor κ-light-chain-enhancer of activated B cells) and IL (interleukin)-4 in the SOT group compared with CON. SOT (n=8 with 5 female and 3 male); CON (n=8 with 4 male and 4 female). Each variable was analyzed by an unpaired *t* test (parametric data) or Mann-Whitney *U* test (nonparametric data).

Sotagliflozin Positively Enhanced Ischemic Myocardial Metabolism

Based on our integration of the proteomic and metabolomic data sets, we discovered enhancement of multiple metabolic pathways, including glycolysis/gluconeogenesis, pyruvate metabolism, the citric acid (tricarboxylic acid [TCA]) cycle, fatty acid degradation, branched-chain amino acid metabolism, nitrogen metabolism, and the urea cycle (Figure 7A and 7C). This is concordant with immunoblotting findings, demonstrating increased expression of GLUT4 (glucose transporter 4), HK2 (hexokinase 2), and CPT1β (carnitine O-palmitoyltransferase 1β) in sotagliflozin swine compared with control (all $P<0.05$; Figure 7B). The increased expression of GLUT 4, the insulin-sensitive glucose transporter, and HK2, the rate-limiting enzyme that phosphorylates glucose on cellular uptake, indicates enhanced glycolytic flux. The upregulation of pyruvate metabolism suggests increased entry of glycolytic products into the TCA cycle. Additionally, the increased expression of CPT1β, a key mitochondrial enzyme involved in fatty acid β-oxidation, aligns with the enrichment of fatty acid degradation pathways. Furthermore, we observed upregulation of propenoate and butanoate metabolism, representing an alternative pathway of short-chain fatty acid oxidation. Figure 7C depicts these global changes in the metabolic pathways of sotagliflozin swine compared with the control. Lastly, rate-pressure product, a simple and reliable surrogate for myocardial oxygen consumption, was calculated and showed no difference between groups ($P=0.24$; Table S1).

The overall proteomic results and pathway enrichment analysis are illustrated in Figure S2. The metabolomic pathway analysis is depicted in Figure S3. The full list of KEGG pathways with ≥1 matched feature from the integration of proteomic and metabolomic data sets is listed in Table S2.

Renal SGLT1 and SGLT2 Expression Following Sotagliflozin Treatment

Kidney tissue staining was performed to determine SGLT1 and SGLT2 abundance and the potential effect of sotagliflozin. Both cotransporters were broadly

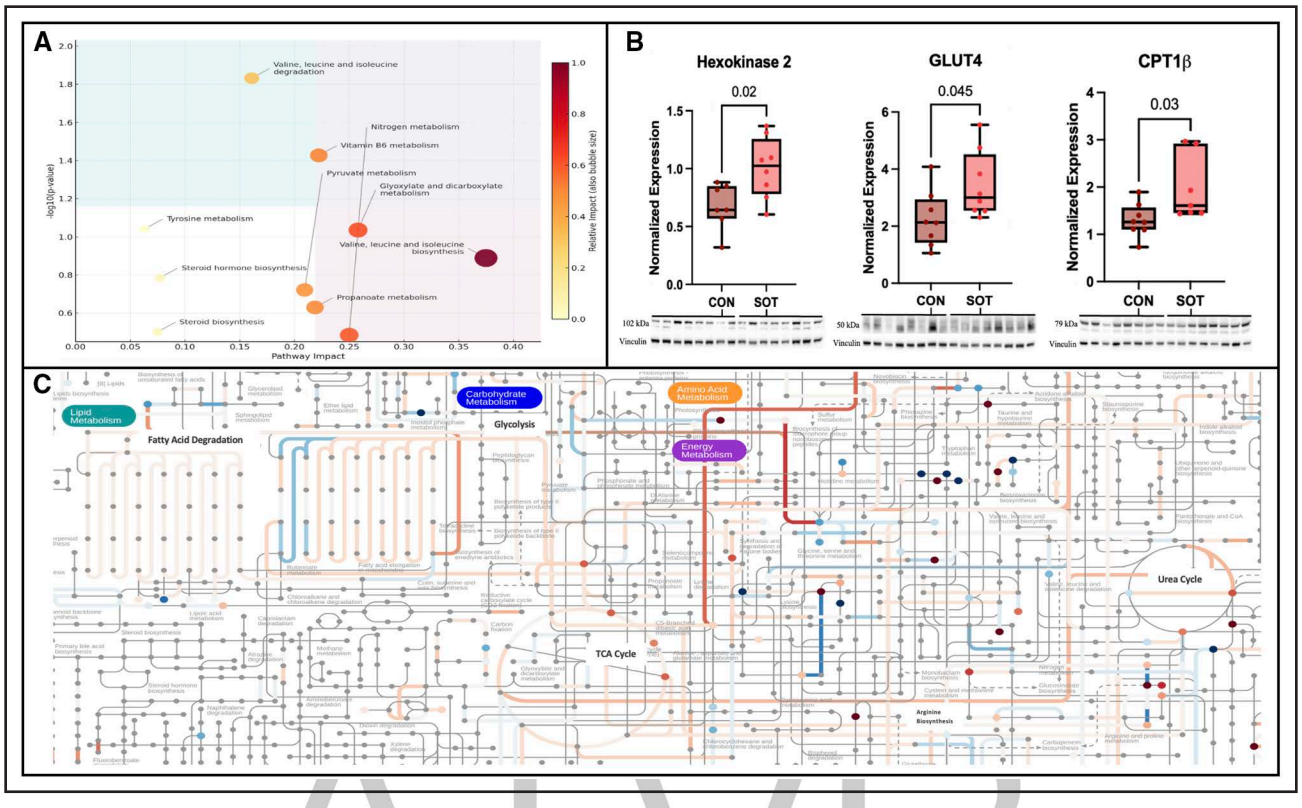

Figure 7. Metabolic remodeling in sotagliflozin (SOT)-treated ischemic myocardium.
A, Integrated proteomic-metabolomic pathway enrichment (MetaboAnalyst). Top enriched pathways include nitrogen metabolism, pyruvate metabolism, branched-chain amino-acid (BCAA) metabolism (specifically valine, leucine, and isoleucine), short-chain fatty-acid (propanoate) metabolism, and steroid biosynthesis. The plot shows pathway impact versus $-\log_{10}$ (*P* value), bubble size, and color scale with impact. **B**, Immunoblot quantification with representative blots: increased HK2 (hexokinase 2), GLUT4 (glucose transporter 4), and CPT1β (carnitine palmitoyltransferase-1β) expression in SOT vs control (CON; normalized to vinculin and *P* values shown), consistent with enhanced glycolytic flux and mitochondrial fatty-acid β-oxidation. These variables were analyzed with an unpaired *t* test. **C**, Global metabolic map (iPath) illustrating coordinated up- (red) and down- (blue) regulation across carbohydrate, lipid, amino acid, and energy metabolism, highlighting increased flux through glycolysis, pyruvate entry to the tricarboxylic acid (TCA) cycle, fatty-acid degradation, and anaplerotic amino-acid pathways.

localized to the proximal tubules in sotagliflozin and control swine, with no difference in SGLT1 or SGLT2 expression between groups (*P*=0.87, *P*=0.13; respectively; Figure 8).

DISCUSSION

Given the recency and clinical promise of dual SGLT1/2 inhibition on ischemic cardiovascular disease, this study provided novel corroborating evidence of overall cardiac benefit without comorbid conditions, and critical insights into the mechanistic determinants of treatment. We found in our clinically translational model of chronic myocardial ischemia that treatment with sotagliflozin improved systolic and diastolic cardiac function as well as myocardial perfusion to the ischemic territory. At the tissue and cellular level, sotagliflozin treatment was associated with (1) increased eNOS expression with concurrent augmentation of arginine metabolism; (2) reduced AMPK activation and signaling; (3) reduced reactive nitrogen species and increased expression of antioxidant enzymes; and (4) attenuated myocardial fibrosis and inflammation due to decreased expression of NFκB, IL-4, and FHL1. The cellular shifts seem to be largely induced by direct myocardial SGLT1 inhibition, as evident by widespread myocardial staining; however, systemic and renal SGLT2 inhibition likely contributed. Furthermore, multiomic analysis revealed significant augmentation of glycolysis, pyruvate metabolism, the TCA cycle, fatty acid degradation, branched-chain amino acid metabolism, and the urea cycle within the ischemic myocardium.

The improvement in overall left ventricular systolic functioning as well as diastolic relaxation after sotagliflozin treatment in our model provided crucial findings to fill a significant scientific knowledge gap. Our model provided clinically translational cardiac physiological and molecular parallels to human patients, especially those with IHD without co-morbid conditions, which accounts for about 20% to 30% of patients.[32,33] Moreover, several preclinical studies have found similar cardiac benefits; however, they typically model acute ischemia or pressure overload.[34,35] To our knowledge, this study represents the first to illustrate overall cardiac benefit in a model of

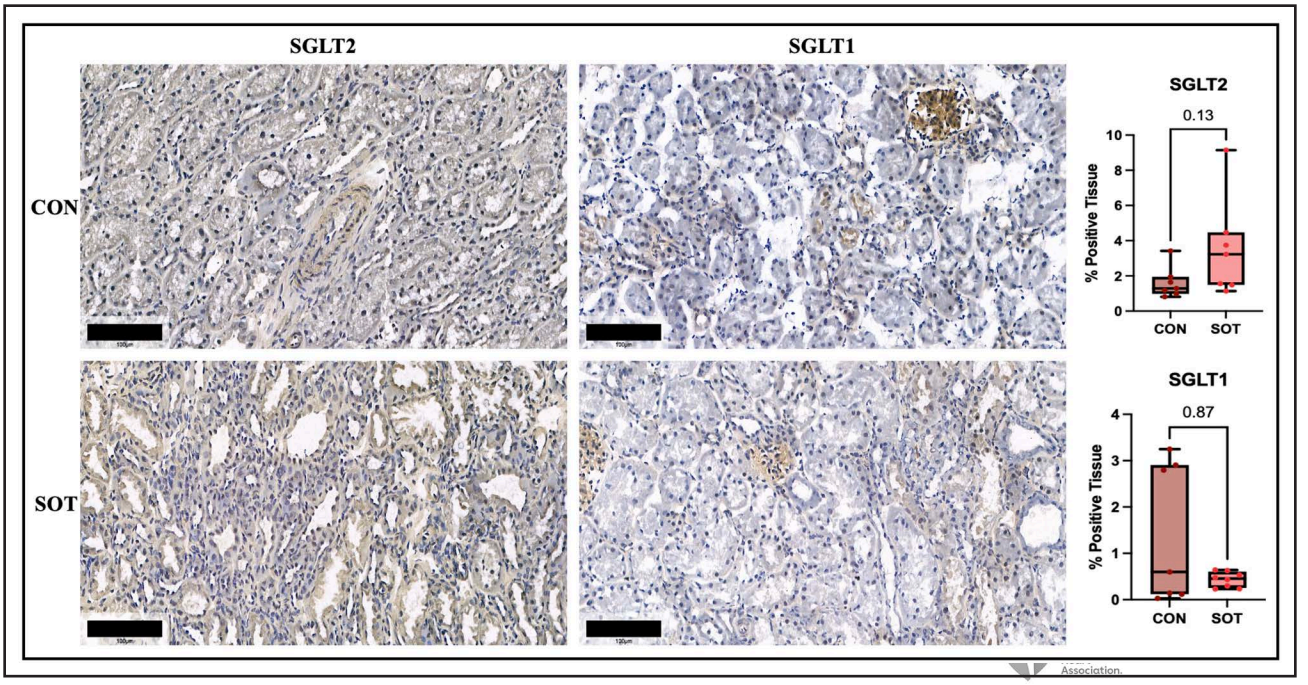

Figure 8. Renal SGLT1 (sodium-glucose cotransporter 1) and SGLT2 (sodium-glucose cotransporter 2) expression.
Immunohistochemistry of SGLT1 and SGLT2 expression in the renal tissue of sotagliflozin (SOT) and control (CON) swine (scale bars=100 µm). There was no difference in expression of either cotransporter between groups, determined by an unpaired *t* test.

chronic IHD, highlighting a critical patient population. For example, Zhong et al[35] demonstrated improved cardiac function and reduced infarct size in a rat model of acute myocardial infarction using left anterior descending artery ligation. Importantly, prior studies support a reduction in left ventricular remodeling and fibrosis attributable to sotagliflozin treatment. Clinically, we observed these findings within the sotagliflozin-treated swine that demonstrated significantly improved diastolic relaxation. Specifically, there was a reduction in the isovolumic relaxation constant, the time constant of isovolumetric relaxation, indicating the ventricle relaxed more efficiently during diastole. Correspondingly, we found an increase in the maximum derivative of volume and minimum derivative of power, suggestive of enhanced ventricular filling and faster reduction in left ventricular pressure during diastole. Overall, the diastolic augmentation may be more revealing than the left ventricular systolic improvement, given that progression to heart failure often begins with diastolic dysfunction.[36] The augmentation of diastolic function after treatment appeared attributable to a reduction in myocardial fibrosis within the ischemic myocardium, likely mediated by dampening NFκB-linked inflammatory signaling with reduced IL-4 levels and the downregulation of FHL1 and ANKRD1/2. These cellular changes within the myocardium have been found to reduce fibroblast activation, fibrogenic cytokine production, collagen deposition, and maladaptive mechanical stress responses.[30,31,37] Studies indicate that the myocardial antifibrotic and anti-inflammatory effects are primarily mediated by direct myocardial SGLT1 inhibition.[38,39] Meanwhile, renal SGLT2 inhibition, which improves glycemic control and provides renoprotective effects, likely augmented these benefits, even without measurable changes in renal SGLT2 expression, a finding consistent with prior studies of SGLT2 inhibitors.[40,41]

Furthermore, sotagliflozin treatment increased absolute myocardial blood flow to the ischemic territory. Notably, the increase in perfusion was not accompanied by improved collateralization—specifically, there was no significant change in capillary or arteriolar densities. Instead, the ischemic-to-nonischemic perfusion ratio was higher in sotagliflozin swine, suggesting the reduction in myocardial fibrosis, together with improved vascular reactivity, resulted in reduced microvascular resistance within the ischemic territory. Notably, an alternative explanation for the increased perfusion was collateral flow from adjacent coronary territories; demonstrating this would require high-resolution angiography, which was not available in this current study. Previous work from our laboratory has shown that the SGLT2 inhibitor, canagliflozin, increased coronary arteriolar vasodilation and decreased vasoconstriction in a swine and rat model of IHD.[42,43] This resulted in similar increased perfusion to the ischemic territory without changes in collateralization. Interestingly, the improvement in microvascular reactivity was found to be endothelial-independent, and local ischemic tissue demonstrated a reduction in renin-angiotensin signaling, which points to myocardial fibrosis as the primary cause.[42] Although endothelial-independent fibrotic changes are likely contributing to the increased perfusion in our current study, we additionally found that sotagliflozin-treated

swine demonstrated increased eNOS expression, although this was not accompanied by a significant rise in eNOS activation via phosphorylation. Moreover, AMPK activation and signaling were reduced, and PI3K-Akt activity remained unchanged—both key components of the canonical kinase pathway responsible for eNOS phosphorylation at Ser1177. However, we observed elevated PKA and cAMP signaling in the sotagliflozin group, providing an alternative route for eNOS activation. PKA can stimulate eNOS by phosphorylating Ser1177 or Ser633, or by removing the inhibitory phosphate at Thr495.[44] These findings suggest that sotagliflozin may enhance eNOS activity through PKA/cAMP-mediated mechanisms rather than the classical AMPK or PI3K-Akt pathways, warranting further investigation into the drug's unique effects on endothelial signaling.

Our findings suggest that sotagliflozin enhanced noncanonical regulation of nitric oxide (NO) production and bioavailability by reducing nitrosative stress, prolonging NO half-life, and increasing substrate availability. These effects are supported by reduced 3-NT staining, elevated expression of SOD3, and augmented arginine metabolism. Reduced 3-NT reflects decreased peroxynitrite formation, generated when NO reacts with superoxide, indicating improved eNOS coupling and less NO scavenging. Increased SOD3 would further reduce levels of peroxynitrite by dismutating superoxide. Mechanistically, preclinical studies have linked SGLT1 protein expression in myocardium to levels of nitrogen-based oxidative stress, suggesting that direct myocardial SGLT1 inhibition played a crucial role.[45] However, the pleiotropic effects of renal SGLT2 inhibition, confirmed by its expression on immunohistochemistry, likely contributed to the observed benefits through reduced glucotoxicity and enhanced diuretic and natriuretic effects.[41,46] Enhanced arginine metabolism provides additional substrate for NO synthesis.[47] We also observed increased levels of 1-methylnicotinamide, a product of nicotinamide metabolism, which has been shown to restore eNOS function by normalizing the NO-to-superoxide balance, thereby improving NO bioavailability and microvascular vasorelaxation.[28] Collectively, these molecular changes likely enhanced coronary arteriolar vasodilation and reduced the need for further activation of eNOS.

A key focus of our study was to evaluate the mechanistic determinants underlying the cardioprotective effects of sotagliflozin, particularly in light of the prevailing hypothesis that other drugs within its class mediate their effects by off-target SGLT1 inhibition. Crucially, we observed global left ventricle staining of SGLT1 in the myocardium, confirming that on-target inhibition likely plays a central role, and is consistent with literature demonstrating SGLT1 is the predominant cardiac isoform.[10] Although mean SGLT1 receptor expression in the ischemic myocardium did not differ between groups, sotagliflozin-treated ischemic SGLT1 expression showed a strong negative correlation with the ischemic-to-nonischemic perfusion ratio, indicating that higher relative perfusion of the ischemic territory corresponded to lower SGLT1 expression. Consistent with this pattern, SGLT1 in the nonischemic myocardium was downregulated after treatment. These findings support the notion that improved microvascular conductance at rest was associated with attenuation of ischemia-responsive SGLT1 expression and maladaptive responses. However, the absence of a significant reduction in ischemic SGLT1 expression may reflect the short treatment interval, limited flow reserve (no perfusion difference at pacing) that sustained intermittent stress, and delayed downregulation despite the overall improved myocardial environment, or ischemia-induced shifts in membrane trafficking.[48] Notably, this is associative and does not establish causality; therefore, future studies utilizing a lengthened treatment window, assessing regional drug exposure, and determining surface versus total SGLT1 expression will clarify this mechanism. Further hypothesis-driven mechanisms for SGLT1 inhibition often cite its ability to reduce cardiac fibrosis and oxidative stress by decreasing AMPK-ERK-mediated upregulation of SGLT1 as well as enhancing metabolic and mitochondrial function.[49] Similarly, we observed a reduction in AMPK signaling and activation. Initially, the downregulation of AMPK may appear counterintuitive in that a multitude of studies have found its activation to be protective in times of myocardial stress or ischemia.[50] However, in a recent study using an ischemia/reperfusion injury in mice, Li et al[51] illustrated that this injury pattern resulted in the upregulation of SGLT1, which was facilitated by AMPK activation. Furthermore, its inhibition was able to reverse this overexpression and subsequent increase in oxidative stress. We propose that direct myocardial SGLT1 inhibition decreases AMPK activity, which could subsequently suppress myocardial SGLT1 expression through a feedback mechanism.

Additionally, sotagliflozin treatment was associated with improved systemic glycemic control and augmentation of ischemic myocardial metabolism, which likely resulted from both renal SGLT2 inhibition and direct myocardial SGLT1 inhibition. Even in a normoglycemic model, insulin sensitivity was improved, as demonstrated by glucose tolerance testing, as well as myocardial glucose handling and expanded substrate utilization. Multiomic analysis of ischemic myocardium revealed upregulation of glycolysis, pyruvate metabolism, the TCA cycle, fatty acid degradation, and branched-chain amino acid metabolism, consistent with immunoblotting results showing increased expression of GLUT4, HK2, and CPT1β. Enhanced glycolytic and TCA cycle activity suggests that the ischemic myocardium was better able to oxidize glucose and generate ATP through aerobic pathways, potentially facilitated by increased perfusion. Moreover, augmentation of alanine, aspartate, glutamate, and branched-chain amino acid metabolism

supports increased mitochondrial TCA activity by replenishing key intermediates. Concurrent increases in fatty acid degradation and CPT1β expression indicate upregulated mitochondrial long-chain fatty acid import and oxidation, although targeted cellular assays are warranted to verify effects on mitochondrial function. This dual enhancement of carbohydrate and lipid oxidation likely reflects restored metabolic flexibility, enabling the ischemic myocardium to draw on multiple substrates to meet energy demands. Furthermore, rate pressure product, a surrogate for myocardial oxygen consumption,[52] was similar between sotagliflozin and control, suggesting the augmentation of ischemic myocardial metabolism in sotagliflozin swine was unlikely to be a demand-driven artifact. However, measuring serum ketone and lactate levels, together with direct measurements of myocardial oxygen consumption, would clarify the extent to which systemic substrate availability and demand versus intrinsic myocardial remodeling drove the observed metabolic changes. Alternatively, given that the healthy heart preferentially relies on fatty acid oxidation, the improved perfusion may have mitigated the ischemic insult, allowing the myocardium to revert toward its primary fuel source.[53] Collectively, the metabolic adaptations suggest that sotagliflozin optimized substrate utilization, matched energy supply to demand under ischemic conditions, and reduced ischemia-induced metabolic bottlenecks.

Limitations

This study provided an insightful view on the cardioprotective benefits and mechanistic reasons behind dual SGLT1/2 inhibition; however, there were limitations that must be considered. As previously discussed, the observation of increased myocardial perfusion without changes in collateralization warrants further investigation into coronary microvascular reactivity. This represents a significant limitation of the project and illustrates an important future study to determine sotagliflozin's influence on the microvasculature and the underlying mechanisms. The overall juvenile swine model provides high anatomic and physiological fidelity to the human cardiovascular system; however, it lacks the complexity of age-related and metabolic changes of chronic disease, representing a limitation in the generalizability of our findings. Future studies utilizing swine with diet-induced metabolic syndrome are underway to more reliably mimic the typical clinical context and compare the therapeutic response under this stressor.

Furthermore, the treatment interval was relatively short. Although it likely would be beneficial and informative to conduct a study with a longer treatment interval, the rapid growth of the swine and desire to maintain a similar heart-to-body size to humans make it challenging to elongate the study. In addition, our study used 1 time point for data collection regarding cardiac function, perfusion, and lacked imaging studies to (1) characterize the area of myocardial ischemia from ameroid placement, ensuring uniformity, and (2) delineate collateral formation. Serial examinations in conjunction with imaging studies, such as cardiac MRI or angiography, would significantly aid in the reproducibility of the model and characterization of the response to therapy. Lastly, because our experiments were conducted in swine, the sample size was relatively small, so further division by sex reduced statistical power, limiting the ability to detect sex-based differences after treatment.

Conclusions

In our clinically translational swine model of IHD, sotagliflozin treatment improved left ventricular systolic function, diastolic relaxation, and myocardial perfusion—even in the absence of comorbidities. These cardiac benefits were driven by distinct cellular adaptations, including improved NO production and bioavailability, reduced nitrogen-based oxidative stress, attenuated myocardial fibrosis and inflammation, enhanced glucose handling, and augmented metabolism in the ischemic myocardium. Together, these findings support a broad cardiometabolic benefit of dual SGLT1/2 inhibition and highlight its therapeutic potential beyond current clinical guidelines.

ARTICLE INFORMATION

Received October 22, 2025; accepted December 4, 2025.

Affiliations

Department of Surgery, Division of Cardiothoracic Surgery, Warren Alpert Medical School, Brown University, Providence, RI (K.C.M., C.S., M.K., D.D.H., M.R.A., F.W.S.). Cardiovascular Research Center, Division of Cardiothoracic Surgery, Rhode Island Hospital, Providence, RI (K.C.M., C.S., R.R., M.K., J.H., D.D.H., M.R.A., F.W.S.).

Acknowledgments

The author would like to extend our sincerest gratitude to our veterinary staff at Rhode Island Hospital and Brown University for their dedication to our investigations and their ongoing ethical care of the animals. Additionally, the author would like to acknowledge the work conducted at the Dana Farber Metabolomic Core and the Brown University Proteomic Core.

Sources of Funding

This project was funded by the National Institutes of Health (NIH) with the following grant numbers: T32HL16051703 (K.C. Muir, D.D. Harris, and C. Stone), R01HL46716 (F.W. Sellke), R01HL128831 (F.W. Sellke), R01HL175045 (M.R. Abid), and R56HL133624-05 (M.R. Abid). M. Kanuparthy was funded in part by the Armand D. Versaci Research Scholar in the Surgical Sciences Award from the Department of Surgery at Brown University. The Brown University Proteomics Core Facility was supported in part by the NIH grant no. 1S10RR027027 (Orbitrap XL-ETD), 1S10OD036295 (Ascend Tribrid, FAIMS, Vanquish Neo), and the Division of Biology and Medicine at Brown University.

Disclosures

None.

Supplemental Material

Figures S1–S3
Tables S1 and S2
Major Resources Table

REFERENCES

1. Nowbar AN, Gitto M, Howard JP, Francis DP, Al-Lamee R. Mortality from ischemic heart disease. *Circ Cardiovasc Qual Outcomes*. 2019;12:e005375. doi: 10.1161/CIRCOUTCOMES.118.005375
2. Virani SS, Newby LK, Arnold SV, Bittner V, Brewer LC, Demeter SH, Dixon DL, Fearon WF, Hess B, Johnson HM, et al; Peer Review Committee Members. 2023 AHA/ACC/ACCP/ASPC/NLA/PCNA guideline for the management of patients with chronic coronary disease: a report of the American Heart Association/American College of Cardiology Joint Committee on Clinical Practice Guidelines. *Circulation*. 2023;148:e9–e119. doi: 10.1161/CIR.0000000000001168
3. Halperin JL, Levine GN, Al-Khatib SM, Birtcher KK, Bozkurt B, Brindis RG, Cigarroa JE, Curtis LH, Fleisher LA, Gentile F, et al. Further evolution of the ACC/AHA clinical practice guideline recommendation classification system: a report of the American College of Cardiology/American Heart Association Task Force on Clinical Practice Guidelines. *Circulation*. 2016;133:1426–1428. doi: 10.1161/CIR.0000000000000312
4. Dauerman HL. Reasonable incomplete revascularization. *Circulation*. 2011;123:2337–2340. doi: 10.1161/CIRCULATIONAHA.111.033126
5. Neal B, Perkovic V, Mahaffey KW, de Zeeuw D, Fulcher G, Erondu N, Shaw W, Law G, Desai M, Matthews DR; CANVAS Program Collaborative Group. Canagliflozin and cardiovascular and renal events in type 2 diabetes. *N Engl J Med*. 2017;377:644–657. doi: 10.1056/NEJMoa1611925
6. Zinman B, Wanner C, Lachin JM, Fitchett D, Bluhmki E, Hantel S, Mattheus M, Devins T, Johansen OE, Woerle HJ, et al; EMPA-REG OUTCOME Investigators. Empagliflozin, cardiovascular outcomes, and mortality in type 2 diabetes. *N Engl J Med*. 2015;373:2117–2128. doi: 10.1056/NEJMoa1504720
7. Bhatt DL, Szarek M, Pitt B, Cannon CP, Leiter LA, McGuire DK, Lewis JB, Riddle MC, Inzucchi SE, Kosiborod MN, et al; SCORED Investigators. Sotagliflozin in patients with diabetes and chronic kidney disease. *N Engl J Med*. 2021;384:129–139. doi: 10.1056/NEJMoa2030186
8. Bhatt DL, Szarek M, Steg PG, Cannon CP, Leiter LA, McGuire DK, Lewis JB, Riddle MC, Voors AA, Metra M, et al; SOLOIST-WHF Trial Investigators. Sotagliflozin in patients with diabetes and recent worsening heart failure. *N Engl J Med*. 2021;384:117–128. doi: 10.1056/NEJMoa2030183
9. Aggarwal R, Bhatt DL, Szarek M, Cannon CP, Leiter LA, Inzucchi SE, Lopes RD, McGuire DK, Lewis JB, Riddle MC, et al. Effect of sotagliflozin on major adverse cardiovascular events: a prespecified secondary analysis of the SCORED randomised trial. *Lancet Diabetes Endocrinol*. 2025;13:321–332. doi: 10.1016/S2213-8587(24)00362-0
10. Sayour AA, Oláh A, Ruppert M, Barta BA, Horváth EM, Benke K, Pólos M, Hartyánszky I, Merkely B, Radovits T. Characterization of left ventricular myocardial sodium-glucose cotransporter 1 expression in patients with end-stage heart failure. *Cardiovasc Diabetol*. 2020;19:159. doi: 10.1186/s12933-020-01141-1
11. Bell RM, Yellon DM. SGLT2 inhibitors: hypotheses on the mechanism of cardiovascular protection. *Lancet Diabetes Endocrinol*. 2018;6:435–437. doi: 10.1016/S2213-8587(17)30314-5
12. Van Steenbergen A, Balteau M, Ginion A, Ferté L, Battault S, de Meester de RC, Balligand J-L, Daskalopoulos E-P, Gilon P, Despa F, et al. Sodium-myoinositol cotransporter-1, SMIT1, mediates the production of reactive oxygen species induced by hyperglycemia in the heart. *Sci Rep*. 2017;7:41166. doi: 10.1038/srep41166
13. Lelovas PP, Kostomitsopoulos NG, Xanthos TT. A comparative anatomic and physiologic overview of the porcine heart. *J Am Assoc Lab Anim Sci*. 2014;53:432–438
14. Suzuki Y, Yeung AC, Ikeno F. The representative porcine model for human cardiovascular disease. *J Biomed Biotechnol*. 2011;2011:195483. doi: 10.1155/2011/195483
15. Stone CR, Harris DD, Broadwin M, Kanuparthy M, Sabe SA, Xu C, Feng J, Abid MR, Sellke FW. Crafting a rigorous, clinically relevant large animal model of chronic myocardial ischemia: What have we learned in 20 years? *Methods Protoc*. 2024;7:17. doi: 10.3390/mps7010017
16. Radke PW, Heinl-Green A, Frass OM, Post MJ, Sato K, Geddes DM, Alton EW. Evaluation of the porcine ameroid constrictor model of myocardial ischemia for therapeutic angiogenesis studies. *Endothelium*. 2006;13:25–33. doi: 10.1080/10623320600660128
17. He X, Gao X, Xie P, Liu Y, Bai W, Liu Y, Shi A. Pharmacokinetics, pharmacodynamics, safety and tolerability of sotagliflozin after multiple ascending doses in Chinese healthy subjects. *Drug Des Devel Ther*. 2022;16:2967–2980. doi: 10.2147/DDDT.S372575
18. Koley S, Chu KL, Gill SS, Allen DK. An efficient LC-MS method for isomer separation and detection of sugars, phosphorylated sugars, and organic acids. *J Exp Bot*. 2022;73:2938–2952. doi: 10.1093/jxb/erac062
19. Mülleder M, Bluemlein K, Ralser M. A high-throughput method for the quantitative determination of free amino acids in saccharomyces cerevisiae by hydrophilic interaction chromatography-tandem mass spectrometry. *Cold Spring Harb Protoc*. 2017;2017:pdb.prot089094. doi: 10.1101/pdb.prot089094
20. Kiefer P, Schmitt U, Vorholt JA. eMZed: an open source framework in Python for rapid and interactive development of LC/MS data analysis workflows. *Bioinformatics*. 2013;29:963–964. doi: 10.1093/bioinformatics/btt080
21. Schmid R, Heuckeroth S, Korf A, Smirnov A, Myers O, Dyrlund TS, Bushuiev R, Murray KJ, Hoffmann N, Lu M, et al. Integrative analysis of multimodal mass spectrometry data in MZmine 3. *Nat Biotechnol*. 2023;41:447–449. doi: 10.1038/s41587-023-01690-2
22. Pang Z, Lu Y, Zhou G, Hui F, Xu L, Viau C, Spigelman AF, MacDonald PE, Wishart DS, Li S, et al. MetaboAnalyst 6.0: towards a unified platform for metabolomics data processing, analysis and interpretation. *Nucleic Acids Res*. 2024;52:W398–W406. doi: 10.1093/nar/gkae253
23. Li S, Park Y, Duraisingham S, Strobel FH, Khan N, Soltow QA, Jones DP, Pulendran B. Predicting network activity from high throughput metabolomics. *PLoS Comput Biol*. 2013;9:e1003123. doi: 10.1371/journal.pcbi.1003123
24. Darzi Y, Letunic I, Bork P, Yamada T. iPath3.0: interactive pathways explorer v3. *Nucleic Acids Res*. 2018;46:W510–W513. doi: 10.1093/nar/gky299
25. Bechmann LE, Emanuelsson F, Nordestgaard BG, Benn M. SGLT2-inhibition increases total, LDL, and HDL cholesterol and lowers triglycerides: meta-analyses of 60 randomized trials, overall and by dose, ethnicity, and drug type. *Atherosclerosis*. 2024;394:117236. doi: 10.1016/j.atherosclerosis.2023.117236
26. Wang D, Gladysheva IP, Fan TH, Sullivan R, Houng AK, Reed GL. Atrial natriuretic peptide affects cardiac remodeling, function, heart failure, and survival in a mouse model of dilated cardiomyopathy. *Hypertension*. 2014;63:514–519. doi: 10.1161/HYPERTENSIONAHA.113.02164
27. Markin SS, Ponomarenko EA, Romashova YA, Pleshakova TO, Ivanov SV, Bedretdinov FN, Konstantinov SL, Nizov AA, Koledinskii AG, Girivenko AI, et al. A novel preliminary metabolomic panel for IHD diagnostics and pathogenesis. *Sci Rep*. 2024;14:2651. doi: 10.1038/s41598-024-53215-9
28. Domagala TB, Szeffler A, Dobrucki LW, Dropinski J, Polanski S, Leszczynska-Wiloch M, Kotula-Horowitz K, Wojciechowski J, Wojnowski L, Szczeklik A, et al. Nitric oxide production and endothelium-dependent vasorelaxation ameliorated by N1-methylnicotinamide in human blood vessels. *Hypertension*. 2012;59:825–832. doi: 10.1161/HYPERTENSIONAHA.111.183210
29. Katz AM. Cyclic adenosine monophosphate effects on the myocardium: a man who blows hot and cold with one breath. *J Am Coll Cardiol*. 1983;2:143–149. doi: 10.1016/s0735-1097(83)80387-8
30. Bogomolovas J, Brohm K, Čelutkienė J, Balčiūnaitė G, Bironaitė D, Bukelskienė V, Daunoravičus D, Witt CC, Fielitz J, Grabauskienė V, et al. Induction of Ankrd1 in dilated cardiomyopathy correlates with the heart failure progression. *Biomed Res Int*. 2015;2015:273936. doi: 10.1155/2015/273936
31. Liang Y, Bradford WH, Zhang J, Sheikh F. Four and a half LIM domain protein signaling and cardiomyopathy. *Biophys Rev*. 2018;10:1073–1085. doi: 10.1007/s12551-018-0434-3
32. Buddeke J, Bots ML, van Dis I, Visseren FL, Hollander M, Schellevis FG, Vaartjes I. Comorbidity in patients with cardiovascular disease in primary care: a cohort study with routine healthcare data. *Br J Gen Pract*. 2019;69:e398–e406. doi: 10.3399/bjgp19X702725
33. van Oostrom SH, Picavet HS, van Gelder BM, Lemmens LC, Hoeymans N, van Dijk CE, Verheij RA, Schellevis FG, Baan CA. Multimorbidity and comorbidity in the Dutch population - data from general practices. *BMC Public Health*. 2012;12:715. doi: 10.1186/1471-2458-12-715
34. Young SL, Ryan L, Mullins TP, Flint M, Steane SE, Walton SL, Bielefeldt-Ohmann H, Carter DA, Reichelt ME, Gallo LA. Sotagliflozin, a dual SGLT1/2 inhibitor, improves cardiac outcomes in a normoglycemic mouse model of cardiac pressure overload. *Front Physiol*. 2021;12:738594. doi: 10.3389/fphys.2021.738594
35. Zhong P, Zhang J, Wei Y, Liu T, Chen M. Sotagliflozin attenuates cardiac dysfunction and remodeling in myocardial infarction rats. *Heliyon*. 2023;9:e22423. doi: 10.1016/j.heliyon.2023.e22423
36. Elgendy IY, Mahtta D, Pepine CJ. Medical therapy for heart failure caused by ischemic heart disease. *Circ Res*. 2019;124:1520–1535. doi: 10.1161/CIRCRESAHA.118.313568
37. Peng H, Sarwar Z, Yang XP, Peterson EL, Xu J, Janic B, Rhaleb N, Carretero OA, Rhaleb NE. Profibrotic role for interleukin-4 in cardiac remodeling and dysfunction. *Hypertension*. 2015;66:582–589. doi: 10.1161/HYPERTENSIONAHA.115.05627
38. Sawa Y, Saito M, Ishida N, Ibi M, Matsushita N, Morino Y, Taira E, Hirose M. Pretreatment with KGA-2727, a selective SGLT1 inhibitor, is protective against

myocardial infarction-induced ventricular remodeling and heart failure in mice. *J Pharmacol Sci*. 2020;142:16–25. doi: 10.1016/j.jphs.2019.11.001
39. Wu W, Chai Q, Zhang Z. Inhibition of SGLT1 alleviates the glycemic variability-induced cardiac fibrosis via inhibition of activation of macrophage and cardiac fibroblasts. *Mol Cell Biol*. 2022;42:e0028221. doi: 10.1128/MCB.00282-21
40. Packer M, Wilcox CS, Testani JM. Critical analysis of the effects of SGLT2 inhibitors on renal tubular sodium, water and chloride homeostasis and their role in influencing heart failure outcomes. *Circulation*. 2023;148:354–372. doi: 10.1161/CIRCULATIONAHA.123.064346
41. Sayour AA, Ruppert M, Oláh A, Benke K, Barta BA, Zsáry E, Merkely B, Radovits T. Effects of SGLT2 inhibitors beyond glycemic control-focus on myocardial SGLT1. *Int J Mol Sci*. 2021;22:9852. doi: 10.3390/ijms22189852
42. Banerjee D, Sabe SA, Xing H, Xu C, Sabra M, Harris DD, Broadwin M, Abid MR, Usheva A, Feng J, et al. Canagliflozin improves coronary microvascular vasodilation and increases absolute blood flow to the myocardium independent of angiogenesis. *J Thorac Cardiovasc Surg*. 2023;166:e535–e550. doi: 10.1016/j.jtcvs.2023.08.017
43. Sabe SA, Xu CM, Sabra M, Harris DD, Malhotra A, Aboulgheit A, Stanley M, Abid MR, Sellke FW. Canagliflozin improves myocardial perfusion, fibrosis, and function in a swine model of chronic myocardial ischemia. *J Am Heart Assoc*. 2023;12:e028623. doi: 10.1161/JAHA.122.028623
44. Bir SC, Xiong Y, Kevil CG, Luo J. Emerging role of PKA/eNOS pathway in therapeutic angiogenesis for ischaemic tissue diseases. *Cardiovasc Res*. 2012;95:7–18. doi: 10.1093/cvr/cvs143
45. Sayour AA, Ruppert M, Oláh A, Benke K, Barta BA, Zsáry E, Ke H, Horváth EM, Merkely B, Radovits T. Left ventricular SGLT1 protein expression correlates with the extent of myocardial nitro-oxidative stress in rats with pressure and volume overload-induced heart failure. *Antioxidants (Basel)*. 2021;10:1190. doi: 10.3390/antiox10081190
46. Zelniker TA, Braunwald E. Mechanisms of cardiorenal effects of sodium-glucose cotransporter 2 inhibitors: JACC state-of-the-art review. *J Am Coll Cardiol*. 2020;75:422–434. doi: 10.1016/j.jacc.2019.11.031
47. Morris SM Jr. Arginine metabolism revisited. *J Nutr*. 2016;146:2579S–2586S. doi: 10.3945/jn.115.226621
48. Banerjee SK, McGaffin KR, Pastor-Soler NM, Ahmad F. SGLT1 is a novel cardiac glucose transporter that is perturbed in disease states. *Cardiovasc Res*. 2009;84:111–118. doi: 10.1093/cvr/cvp190
49. Zhao M, Li N, Zhou H. SGLT1: a potential drug target for cardiovascular disease. *Drug Des Devel Ther*. 2023;17:2011–2023. doi: 10.2147/DDDT.S418321
50. Feng Y, Zhang Y, Xiao H. AMPK and cardiac remodelling. *Sci China Life Sci*. 2018;61:14–23. doi: 10.1007/s11427-017-9197-5
51. Li Z, Agrawal V, Ramratnam M, Sharma RK, D'Auria S, Sincoular A, Jakubiak M, Music ML, Kutschke WJ, Huang XN, et al. Cardiac sodium-dependent glucose cotransporter 1 is a novel mediator of ischaemia/reperfusion injury. *Cardiovasc Res*. 2019;115:1646–1658. doi: 10.1093/cvr/cvz037
52. Gobel FL, Norstrom LA, Nelson RR, Jorgensen CR, Wang Y. The rate-pressure product as an index of myocardial oxygen consumption during exercise in patients with angina pectoris. *Circulation*. 1978;57:549–556. doi: 10.1161/01.cir.57.3.549
53. Shi X, Qiu H. New insights into energy substrate utilization and metabolic remodeling in cardiac physiological adaption. *Front Physiol*. 2022;13:831829. doi: 10.3389/fphys.2022.831829